REMOTE SENSING OF LEAF AREA INDEX IN SAVANNAH GRASS USING INVERSION OF RADIATIVE TRANSFER MODEL ON LANDSAT 8 IMAGERY: CASE STUDY MPUMALANGA, SOUTH AFRICA

BY

CECILIA RAMAKGAHLELE MASEMOLA

Submitted in accordance with the requirements for

the degree of

MASTER OF SCIENCE

in the subject

ENVIRONMENTAL SCIENCE

at the

UNIVERSITY OF SOUTH AFRICA

SUPERVISOR: DR. MOSES AZONG CHO

CO-SUPERVISOR: MR. MARTEN JORDAAN

MARCH 2015

DECLARATION

By submitting this thesis, I declare that "Remote sensing of leaf area index in savannah grass using inversion of radiative transfer model on Landsat 8 imagery: CASE STUDY MPUMALANGA, SOUTH AFRICA**"** is my own work and I am the sole author thereof, that reproduction and publication thereof by University of South Africa will not infringe any third party rights. I also declare that all the sources and quotes used in this study have been acknowledged by means of complete references and that I have not previously in its entirety or in part submitted it for obtaining any qualification.

…… ……..

SIGNATURE DATE

(Mrs. Cecilia Ramagahlele Masemola).

ACKNOWLEGEMENTS

This thesis would never have been possible without the stimulating suggestions and encouragement of my supervisor Dr Moses Azong Cho, who helped me to coordinate the study, especially with modeling aspects, data analysis and the writing of this thesis. Furthermore, I would like to thank him for his patience, comments and constructive criticism because I have profited a lot when comes to conducting research studies. A special gratitude I give to Dr Abel Ramoelo who invested his full effort in guiding me in achieving the goal of this research study, particularly his valuable suggestions regarding analysis aspects of my thesis. Thanks also go to my co-supervisor Mr Maarten Jordaan from University of South Africa for assisting with administrative site of this thesis. Also I would like to thank Dr Roshanak Darvishzadeh for clarifying some of the things I did not understand on modeling aspects.

Furthermore, I would also like to acknowledge with much appreciation the crucial role of the Earth Observation, Natural Resources and Environment, Council for Scientific and Industrial Research (CSIR) group that gave the support and permission to use all required equipment and the necessary material required for field work and data processing as well as data analysis. Also, I owe thanks to Mr Oupa Malahlele for helping me during field data collection. Another appreciation goes to Ms Heidi van Deventer for sharing her bootstrap script used for regression analysis.

Finally, I am grateful to my family for the unconditional support and encouragement they have given me, my mother, Ramatsobane Mulukwane for her support and blessings. To my dear and loving husband, Jacob Matuba Masemola I would like to thank you for your endless support and encouragement throughout this study. To my sons, Tumelo and Moeketsi thank you for understanding.

I express my gratitude to the National Research Foundation (NRF) free standing MSc scholarship and University of South Africa (UNISA) post graduate scholarship funding for all the financial support granted throughout my MSc programme.**THANK YOU ALL!**

ABSTRACT

Savannahs regulate an agro-ecosystem crucial for the production of domestic livestock, one of the main sources of income worldwide as well as in South African rural communities. Nevertheless, globally these ecosystem functions are threatened by intense human exploitation, inappropriate land use and environmental changes. Leaf area index (LAI) defined as one half the total green leaf area per unit ground surface area, is an inventory of the plant green leaves that defines the actual size of the interface between the vegetation and the atmosphere. Thus, LAI spatial data could serve as an indicator of rangeland productivity. Consequently, the accurate and rapid estimation of LAI is a key requirement for farmers and policy makers to devise sustainable management strategies for rangeland resources.

In this study, the main focus was to assess the utility and the accuracy of the PROSAILH radiative transfer model (RTM) to estimate LAI in the South African rangeland on the recently launched Landsat 8 sensor data. The Landsat 8 sensor has been a promising sensor for estimating grassland LAI as compared to its predecessors Landsat 5 to 7 sensors because of its increased radiometric resolution. For this purpose, two PROSAIL inversion methods and semi- empirical methods such as Normalized difference vegetation index (NDVI) were utilized to estimate LAI. The results showed that physically based approaches surpassed empirical approach with highest accuracy yielded by artificial neural network (ANN) inversion approach (RMSE=0.138), in contrast to the Look-Up Table (LUT) approach (RMSE=0.265). In conclusion, the results of this study proved that PROSAIL RTM approach on Landsat 8 data could be utilized to accurately estimate LAI at regional scale which could aid in rapid assessment and monitoring of the rangeland resources.

Keywords: Leaf area index (LAI), Radiative Transfer Models, PROSAIL, LUT, ANN, Vegetation Indices, Empirical methods, Landsat 8 imagery.

TABLE OF CONTENTS

LIST OF ACRONYMS

ACRM	-	A two-layer canopy reflectance model
ALA	-	Average leaf angle
ANN	-	Artificial Neural Network
ASD	-	Analytical Spectral Devices
ASTER	-	Advanced Spaceborne Thermal Emission and Reflection
AVIRIS	-	Airborne visible /Infrared Imaging Spectrometer
AWiFS	-	Advanced wide field sensor
CHRIS	-	Compact High Resolution Imaging Spectrometer
ENVI	-	ENvironment for Visualizing Images
GARI	-	Green Atmospherically Resilient Index
GIPVI	-	Green Infrared Percentage Vegetation Index
GOSAVI	-	Green optimized soil adjusted vegetation index
GSAVI	-	Green soil adjusted vegetation index
LAI	-	Leaf Area Index
LUT	-	Look-up table
MATLAB	-	Matrix Laboratory

MSE	-	Mean square error
MERIS	-	Medium Resolution Imaging Spectrometer
MODIS	-	Moderate-resolution Imaging Spectroradiometer
NDVI	-	Normalized Difference Vegetation Index
NIR	-	Near Infrared Reflectance
NNIR	-	Normalized Near Infrared
NOP	-	Numerical optimization approach
NR	-	Normalized Red
OPT	-	Iterative optimization technique
PCA	-	Principal Component Analysis
PCI	-	Principal Component Inversion
PVI	-	Percentage vegetation index
PLSR	-	Partial least square regression
R^2	-	Coefficient of determination
RF	-	Random Forest
RMS	-	Root Mean Square
RMSE	-	Root Mean Square Error
RTM	-	Radiative Transfer Model
RS	-	Remote sensing
SAIL	-	Scattering from Arbitrarily Inclined Leaves
SAVI	-	Soil Adjusted Vegetation Index
SMLR	-	Stepwise multiple linear regression
SR	-	Simple ratio
SVM	-	Support Vector Machine
SPOT	-	Système Pour l'Observation de la Terre
TM	-	Thematic Mapper
TRAC	-	Tracing Radiation and Architecture of Canopies (instrument)
TSAVI	-	Transformed Soil Adjusted Vegetation Index
UAV	-	Unnamed aerial vehicle

UTM - Universal Transverse Mercator

VIs - Vegetation Indices

LIST OF FIGURE

LIST OF TABLES

Chapter 1. Introduction and background of the study

Savannahs are ecosystems characterized by scattered trees found in transition zones between forest and grasslands. Savannahs occupy nearly 20% of the Earth's surface, and half of the savannahs are found on the African continent (Sankaran and Anderson 2008). In South Africa, they occupy 32.8% of the land (Mucina and Rutherford 2006; Ramoelo et al. 2012). Globally, savannah ecosystems have a profound impact on the rural community's livelihood, biogeochemical fluxes and climate (Dickinson et al. 1986; Melillo et al. 1993). For instance, they regulate an agro-ecosystem crucial for the production of domestic livestock, one of the main sources of income worldwide as well as in South African rural communities (Ramoelo et al. 2012). Africa's rangelands supply most of the beef and milk requirements of the African continent (Reid 2004; Marchant 2010). In South Africa, 50% of the country's beef cattle are farmed in the grasslands. Nevertheless, globally these ecosystem functions are threatened by intense human exploitation, inappropriate land use and environmental changes (He and Mui 2010). This could lead to undesirable impacts on the rural economy of the country and worldwide (Shackleton et al. 2002; James et al. 2003; Ramoelo et al. 2012). Furthermore, altered savannah ecosystems can also result in loss of native habitat, bush encroachment, decline of species diversity and alteration of soil dynamics (Olson 1999). Therefore, regional information about grasslands biophysical parameters is crucial for sustainable monitoring of the rangeland resources by farmers, resource managers and land use planners (Ramoelo et al. 2012).

To accurately monitor rangeland resources, measurements of a key structural characteristic of vegetation called leaf area index (LAI) are required at various spatial scales (He and Mui 2010). LAI defined as one half the total green leaf area per unit ground surface area (Jonckheere et al. 2004), is an inventory of the plant green leaves that defines the actual size of the interface between the vegetation and the atmosphere Consequently, it plays a major role in spatially distributed modelling of surface energy balance,

evapotranspiration and vegetation productivity. For instance, LAI spatial data could serve as an indicator of rangeland productivity. Thus accurate information on the variability of rangelands LAI at the regional scale is required for routine assessment and monitoring of rangeland productivity. Such information could help stakeholders such as park managers, farmers, planning managers and policy makers to devise sustainable management strategies for rangeland resources. Thus increase livestock productivity, crucial for rural community economy of the country, as well as reduce inappropriate usage of rangelands. Conventionally, the estimation of LAI is done through field surveys using direct and indirect ground-based methods (Welles 1990; Breda 2003; Jonckheere et al. 2004). However, the methods are labor and time consuming (Gobron et al. 1997; He et al. 2006) and uneconomical (Darvishzadeh et al. 2012). Thus, hardly applicable in case of larger scale ecosystems such as savannahs. Consequently, most studies have resorted to remote sensing technology for economical and rapid means of estimating variation of LAI on larger scale.

Traditionally, empirical or statistical approaches that involve the establishment of the empirical relationship between the target variable (in this case LAI) and vegetation indices (VIs) (Darvishzadeh et al. 2008a; 2010) have been utilized. The Normalized Difference Vegetation Index (NDVI) (Chen and Cihlar 1996; Myneni et al. 1997b; Hassan and Bourque, 2010; Viña et al. 2011) and different regression techniques such as neural network (Jensen & Hardin 2005; Bajwa et al. 2008), Partial Least Square Regression (Darvishzadeh et al. 2008) and fusion technique (Hassan and Bourque 2010) have been used to estimate LAI.

Although VI (e.g. NDVI) has shown a satisfactory relationship with LAI, Gitelson et al. (2004) and Gonzalez-Sanpedro et al. (2009) reported insensitivity of NDVI to high LAI values. In addition, Gonzalez-Sanpedro et al. (2009) observed the effect of plant structure and leaf properties on LAI- NDVI relationships. On the other hand, Turner et al. 1999; Weiss et al. 2000; Boegh et al. 2002; Gitelson et al. 2005, reported sensitivity of VIs to the vegetation developmental stage, geometry of observation and understory vegetation. Furthermore, the models suffer from collinearity and over-fitting as well as being

site-specific and non-transferable (Vuolo et al. 2013). Thus, it is challenging to use empirical methods on savannah given the heterogeneity and scale of the ecosystem.

Alternatively, physically-based RTMs have displayed flexibility in retrieving LAI on heterogeneous grassland. The models involve the combination of leaf and canopy reflectance models to describe the transfer and interactions of radiation inside the canopy based on physical laws. The most validated RTM models are 1-Dimensional (1-D) leaf reflectance model called PROSPECT (Jacquemoud & Baret 1990) and canopy reflectance model known as SAIL (Verhoef 1985) combined to form PROSAIL (Jacquemoud and Baret 1993). However, validation was done mainly on homogeneous vegetation (e.g. agricultural crops, González-Sanpedro et al. 2007; Tripathi et al. 2009; Nguyen et al. 2013 and Nigam et al. 2014). Only few studies have evaluated inversion of the PROSAIL RTM on heterogeneous grasslands and it was mainly on the European grasslands. For example, Darvishzadeh et al. 2008a applied PROSAIL inversion on the Mediterranean grassland of Majella National Park in Italy, Si et al. (2012) in the grasslands of Netherland and Vohland and Jarmer (2008) on heterogeneous grassland in Germany. The above mentioned studies demonstrated the potential of RTM inversion for accurate estimation of LAI on heterogeneous grasslands. Yet, there is no study for assessing the utility of these models on South African heterogeneous grasslands. Therefore, it is critical to assess the potential and accuracy of RTM of retrieving LAI in South African grasslands. Accurate estimates of LAI could be useful in providing essential information for sustainable planning and management of South African rangeland resources by farmers, resource managers and land use planners (Ramoelo et al. 2012).

Savannah landscape is heterogeneous (multiple species) and often composed of non-vegetated areas and dead litter (He at al. 2006). As a result, the SAIL model may not be applicable because of clumping effects which can lead to bias in the target biophysical parameter (Meroni et al. 2004; Darvishzadeh et al. 2008). Conversely, when stratified according to dominant species, PROSAIL has been able to estimate LAI of heterogeneous grassland (e.g. montane system in Italy (Darvishzadeh et al. 2008a). Furthermore, this can also be surmounted by estimating LAI during peak grass productivity, because heterogeneity is

less if not visible. Moreover, these studies were performed with Hyperspectral (Darvishzadeh et al. 2008a; Vohland and Jarmer 2010) and multi-temporal (Si et al. 2012) satellite images. So far, no study is available in which inversion of PROSAIL RTM on multispectral satellite image in particular Landsat 8 data has been evaluated for the estimation of LAI in heterogeneous grassland. This makes it all the more important to assess the potential of PROSAIL inversion for LAI estimation on Landsat 8 data. Furthermore, the new Landsat 8 has a higher radiometric resolution than its predecessors, Landsat 5 to 7 sensors. The accuracy of the models was compared to the semi-empirical models.

The specific objectives of this study were to:

1. Investigate if PROSAIL RTM can be used to accurately estimate LAI in a heterogeneous savannah grassland ecosystem at peak productivity using multispectral RS data. PROSAIL is the combination of PROSPECT (a leaf RTM) and SAIL (a canopy reflectance model) (Jacquemoud and Baret 1993).

2. Assess the accuracy of the RTM model in comparison with empirical methods in estimating LAI.

3. Assess the accuracy of Landsat 8 data compared to *in situ* LAI measurements.

And the main questions are:

1. Can radiative transfer model be used to accurately retrieve grassland LAI from Landsat 8 imagery?

2. How accurate are RTMs compared to empirical modelling for estimation of LAI?

Chapter 2: Review of study

2.1. Ground-based LAI estimation methods

Traditionally spatial variability of LAI has been measured through: (1) Ground-based methods, and (2) Remote sensing methods. The ground-based methods are categorized into: (1) Direct ground-based-methods and (2) Indirect ground-based methods. The direct method involves harvesting of green leaves from the sample plot and building a statistical relationship between the individual leaf area and the number of area units covered by that leaf in a horizontal plane (Jonckheere et al. 2004) using either planimetric or gravimetric techniques. The method was used by Stroppiana et al. (2006) to estimate LAI of rice in Northern Italy. Furthermore, Casanova et al. (1998) and Sarlikioti et al. (2011) measured LAI directly using a LI-300 Area Meter. On the other hand, indirect ground-based methods involve the use of ground-based optical instruments such as LAI-2000 Plant Canopy Analyzer and digital hemispheric photography (Schiffman et al. 2008). LAI-2000 Plant Canopy Analyzer measures the diffused sunlight at various zenith angles ranges based on the canopy gap fraction or gap size distribution (Wittamperum et al. 2012). The LAI is measured by taking measurements at above and below the canopy of vegetation. The high value of LAI represents denser or healthy vegetation, while sparse or drier canopy will be represented by low LAI values. He et al. 2006; Darvishzadeh et al. 2008; Vohland et al. 2010; and Si et al. 2012 measured LAI of European heterogeneous grasslands using LAI-2000 Plant Canopy Analyzer. Liu et al. (2010) indirectly measured LAI of corn, soybean and wheat canopies in Eastern Canada using LAI-2000 Plant Canopy Analyzer. In addition, Friedl et al. (1994) estimated grassland LAI using ground and satellite data. However, these methods are suitable for small sampling areas because they are subjected to errors with the increase in spatial of vegetation canopy such as savannahs. These methods are also laborious and time consuming, making application over large spatial extents, very challenging (Gobron et al. 1997). For that reason, most studies have resorted to remote sensing based techniques for economical and rapid means of estimating spatial and variation of LAI on a larger scale.

2.2. Estimation of the leaf area index from remote sensed data

Remote sensing based methods are an economical and rapid means of estimating spatial and variation of LAI on a larger scale (Darvishzadeh et al. 2008a). Moreover, the methods are spatially explicit, can be scaled from stand to larger extents and could be used to access inaccessible areas (Running et al. 1986). Two main methods are classified into: (I) Empirical or statistical methods (Turner et al. 1999; Xavier & Vettorazzi 2004; He et al. 2006 and Kross et al. 2015) and (II) Physical based RTMs (Bacour et al. 2006; Vohland et al. 2006; Darvishzadeh et al. 2008a; Vohland et al. 2010; Vuolo et al. 2010; Si et al. 2012).

2.2.1 Empirical or statistical methods

In the empirical or statistical approach, regression models are used to acquire a relationship between the target variable and its spectral reflectance (Darvishzadeh et al. 2008a; 2012). The models are categorized into: (1) Univariate regression that relates target variable with either the reflectance at a specific waveband or a spectral index (Majeke et al. 2008) and (2) multivariate regression that relates several spectral bands to estimate biophysical concentrations (Majeke et al. 2008). In addition, the multivariate regression incorporates other independent variables (e.g. surface reflectance data, vegetative indices, climate data and categorical data). Univariate regressions are mostly used for estimating biophysical variables. For instance, various studies have estimated LAI from vegetation indices (Table 2.1) derived from various remote sensed (RS) data (e.g. Table 2.2(*a*) shows VI and results obtained from various studies).

Table 2.1. Difference vegetation indices used for estimation of LAI in previous studies.

VEGETATION INDEX	ACRONYM	FORMULA	REFERENCES
Simple ratio	SR	nIR/red	Jordan, 1969
Normalized Difference Vegetation Index	NDVI	(nIR-red)/(nIR+red)	Rouse et al, 1973
Difference vegetation index	DVI	NIR – red	Tucker, 1979
Green difference vegetation index	GDVI	NIR – green	Sripada et al. 2006

Green Normalized Difference Vegetation Index	GNDVI	NIR – green) / (NIR + green)	Buschmann and Nagel, 1993
Normalized green	NG	Green / (NIR + red + green)	Sripada et al. 2006
Normalized red	NR	Red / (NIR + red + green)	Sripada et al. 2006
Normalized near infrared	NNIR	NIR / (NIR + red + green)	Sripada et al. 2006
Infrared percentage vegetation index	IPVI	NIR / (NIR + red)	Crippen, 1990
Ratio Vegetation Index (also known as the Simple Ratio)	RVI	NIR / red	Birth and McVey, 1968
Green Infrared Percentage Vegetation Index (same as IPVI but using green band instead of red)	GIPVI	NIR / (NIR + green)	Crippen, 1990
Modified simple ratio	MSR	(nIR/red-1)/√ (nIR/red+1)	Chen, 1996
Difference vegetation index	DVI	nIR-red	Richardson et al. 1992
Renormalized difference vegetation index	RDVI	√(NDVI * DVI)	Roujean & Breon, 1995
Green Normalized Difference Vegetation Index	GNDVI	(nIR-green)/(nIR+green)	Gitelson et al. 1996
Soil adjusted vegetation index			
Transformed soil adjusted vegetation index	SAVI	(nIR-red)(1+L)/(nIR*red*L), L=0.5	Huete, 1988
Soil adjusted vegetation index 2	SAVI 2	(nIR-a*red-b)/(red+a*nIR-a*b) line coefficients nIR/(red+a/b)	Baret et al. 1989
Modified soil adjusted vegetation index	MSAVI	nIR+0,5-√((nIR+0,5)2-2*(nIR-red))	Major et al. 1990
Modified soil adjusted vegetation spectral index	MSAVI2	[2*NIR + 1 - √ (2*NIR+1)² - 8*(NIR – red)] / 2	Qi et al. 1994
Green optimized soil adjusted vegetation index	GOSAVI	[(NIR – green) / (NIR + green +L)] * (1 + L)	Cao et al. (2013), modified from Rondeaux et al. (1996)
Enhance vegetation index	EVI	[(NIR – red) / (NIR + C1*red – C2*blue + L)]	Liu and Huete, 1995
Optimized soil adjusted vegetation index	OSAVI	(nIR-red)(1+0.16)/(nIR+red+0.16)	Qi et al. 1994
Generalized soil adjusted vegetation index	GESAVI	nIR-b*red-a/red+0,35	Rondeaux et al., 1996)
Green soil adjusted vegetation index	GSAVI	[(NIR – green) / (NIR + green +L)] * (1 + L), where L = 0.5.	(Gilabert et al. 2002)
Transformed soil adjusted vegetation index	TSAVI	[a (NIR – a*red – b)] / [a*NIR + red – (a*b) + X(1+a²)]	Baret et al. 1989

Atmospherically resilient vegetation indices			
Green atmospherically resilient index	GARI	NIR – [green – (blue – red)] / NIR [green – (blue – red)]	Gitelson et al. 2002
Vegetation index green	VARI green	(green – red) / (green + red - blue)	Gitelson et al. 2002

Li and Guo (2011) reported a relationship between LAI and NDVI in mixed canopies grassland site at Saskatchewan, Canada. Darvishzadeh et al. (2008) reported correlation between LAI and NDVI in Italian heterogeneous grassland. Although these studies and others reported VIs to be correlated with LAI (results extracted from various studies are shown in Table 2.2(*a*), insensitivity of NDVI to LAI greater than three have been observed by Gitelson et al. (2004) and Gonzalez-Sanpedro et al. (2009). In addition, Spanner et al. (1990) and Gonzalez-Sanpedro et al. (2009), observed dependence of NDVI to vegetation type and canopy structure. Whereas, Baret & Guyot (1991); Turner et al. (1999); Weiss et al. (2000) and Boegh et al. (2002), reported sensitivity of VI to vegetation developmental stage, geometry of observation and understory vegetation. In order to correct asymptotic saturation of the vegetation indices, new vegetation indices were developed by incorporating different spectral bands such as soil corrected vegetation indices and chlorophyll corrected VIs. Li and Guo (2011) reported an optimum relationship between LAI and standardized LAI determining index (SLAIDI), and TSAVI, respectively in a mixed canopies grassland site at Saskatchewan, Canada. He et al. (2006) observed improved relationship between heterogeneous grass LAI and L-ATSAVI (formed by incorporating the cellulose absorption index (CAI) as a litter factor in ATSAVI) in Grasslands National Park (GNP) in southern Saskatchewan. Nevertheless, the indices still suffer from the effect of leaf chlorophyll variations on the LAI-vegetation index relationship.

Other studies tested multivariate regression, which involves calibration equation that relates the field measurements of LAI to the spectra. Table 2.2 (*b*) shows the studies and results observed from the approach. These studies observed improved performance as compared to a univariate approach (LAI-VI). For instance, Bajwa el al. (2008) compared artificial neural network and least square regression

techniques for LAI retrieval from Landsat Thematic Mapper (TM), and R^2 value of 0.91 was observed for ANN model and R^2 of 0.84 from univariate regression. On the other hand, Darvishzadeh et al. (2008) demonstrated the improvements of the relationship between measured and estimated LAI when using stepwise multiple linear regressions (SMLR) and partial least square regression (PLSR). The author obtained R^2 of 0.67 (SMLR) and 0.87 (PLSR) for grass as compared to R^2 of 0.60 and 0.63 obtained from VIs method (i.e. narrow band vegetation indices and red edge position index respectively). Chaurasia and Dadhwal, 2004 found that multi-band principal components inversion (PCI) approach yielded a high accuracy (RMSE= 0.380) as compared to NDVI and SR approaches (RMSE=2.28, 0.88). However, these techniques have a weakness for collinearity and over-fitting. In addition, the model is limited to being site-specific and non-transferable. Vuolo et al. (2013) observed limitation of transferability of support vector machine (SVM) and random forest regression (RF) methods. The study reported an increase of RMSE of 24% and 38% for RF and SVM, respectively. Thus general applicability of these methods in savannahs is limited, mainly because of heterogeneity, sparse canopy, litter as well as larger scale.

2.2.2 Physical-based radiative transfer model

Alternatively, physically-based RTMs are more accurate and flexible to apply on a larger scale. As a result, these models receive a rapid development in remote sensing of terrestrial environments (Liang 2007; Mazumdar 2011). RTMs describe the interaction of electromagnetic radiation with plant leaves and canopy (Verhoef 1984). Thus, they model relation between canopy properties and its reflection behaviour and provide values of reflectance from biophysical variables (Urrutia 2010). Although these models are more complex when compared to empirical methods, they are advantageous because they can account for the various sources of variability (Gonzalez-Sanpedro et al. 2009). For instance, they require a wide range of land cover situations and sensor configurations for parameterizing (Delegido et al. 2011). They can be applied to various remote sensing data acquired over the same vegetation cover (Darvishzadeh et al. 2011), thus, overcome the site and sensor specificity problems of

statistical approach. In addition, LAI can be inverted in the high range, overcoming insensitivity of VI to higher LAI values (Gonzalez-Sanpedro et al. 2009).Amongst RTMs, the leaf reflectance model, PROSPECT (Jacquemoud & Baret, 1990) and canopy reflectance model called SAIL (Verhoef 1985) are the most validated to estimate LAI in various biomes. Mostly because of they are less complex when compared to 3D RTMs.

2.2.2.1 PROSPECT

The PROSPECT (Jacquemoud & Baret 1990) is a leaf reflectance model used to simulate leaf optical properties from visible to mid-infrared based on leaf chemical composition. The PROSPECT simulates interaction of rays with leaf surface through Fresnel laws (Gascon et al. 2007). Volume interactions described by the absorption coefficient (k (λ)) is through the Beer-Lambert's law (Gascon et al. 2007). The absorption coefficient (k (λ)) is a function of the chemical concentrations (Shown in Equation 1) which is used in the stacked layer model and results in a leaf reflectance and transmission.

$$k(\lambda) = \sum_i \frac{C_i \, k_i \, \lambda}{N} \qquad \textbf{(Equation 1)}$$

Where λ is a wavelength *(400-2100), C_i a* concentration of constituents (Cab, Car, Brown, Cw and Cm) per leaf surface unit of the biochemical component, k_i is the absorption coefficient specific and N is a leaf structural parameter.

Because the model was developed based on Allen et al. (1969)'s "plate model'', assumes the leaf as a stack of thin 'plates' which differ according to the type of leaf. For instance, monocotyledon leaves are treated as a single plate. The leaf structure parameter (N) is a very important parameter in the model because it is equivalent to leaf layers related to leaf internal complexity. The value for N varies with plant type (monocot and dicot), for instance, according to Jacquemoud and Baret (1990) value of N close to one represents a monocotyledon leaf type. While values between 1.5 and 2.5 represent those of dicotyledons. They further noted that for senescent leaves the value of N is mostly over 2.5 as shown by their internal

structure.

Although the model was designed to return leaf reflectance and transmittance between 400 and 2500 nm with steps of 5nm, with the inclusion of the specific filter function the model can be applied to other data such as multispectral data. In this study the resampling was done and the PROSPECT leaf model matched the Landsat 8 sensor characteristics. Therefore, the PROSPECT model simulated leaf reflectance and transmittance that correspond exactly with the wavelength used by the Landsat 8 sensor. The PROSPECT output is then used as an input to SAIL to simulate canopy reflectance.

2.2.2.2 SAIL

The SAIL (Verhoef, 1984) is the canopy reflectance model used to calculate the bi-directional reflectance factor of a vegetative canopy with inclined leaves (Verhoef et al. 1987 ;Verhoef et al. 2003) as a function of leaf optical properties (such as LAI, Average Leaf Angle (ALA) parameters), measurement conditions (Verhoef, 1984) and of hotspot abbreviated as ‘’H’’ (the peak in the reflectance when the sun is directly behind the sensor (Kuusk 1985; Goel 1983). This model is based on the assumption of homogeneous semi-infinite medium canopy with Lambertian reflecting leaves. Therefore, canopy reflectance is simulated as a homogeneous layer composed of randomly distributed leaves of small size (Jacquemoud et al. 1995). For SAIL to retrieve biophysical parameters, the model must be coupled with leaf reflectance models (PROSPECT) to form PROSAIL (Figure 2.1). Jacquemoud, 1993 was the first to couple leaf level PROSPECT to canopy level SAIL RT model. The study inverted PROSAIL on AVIRIS reflectance spectra. Since then various studies inverted the model to retrieve LAI on various RS data as shown in table 2.3. However, most studies were undertaken on homogeneous vegetation such as agricultural crops and forest (Table 2.3(*a*)).

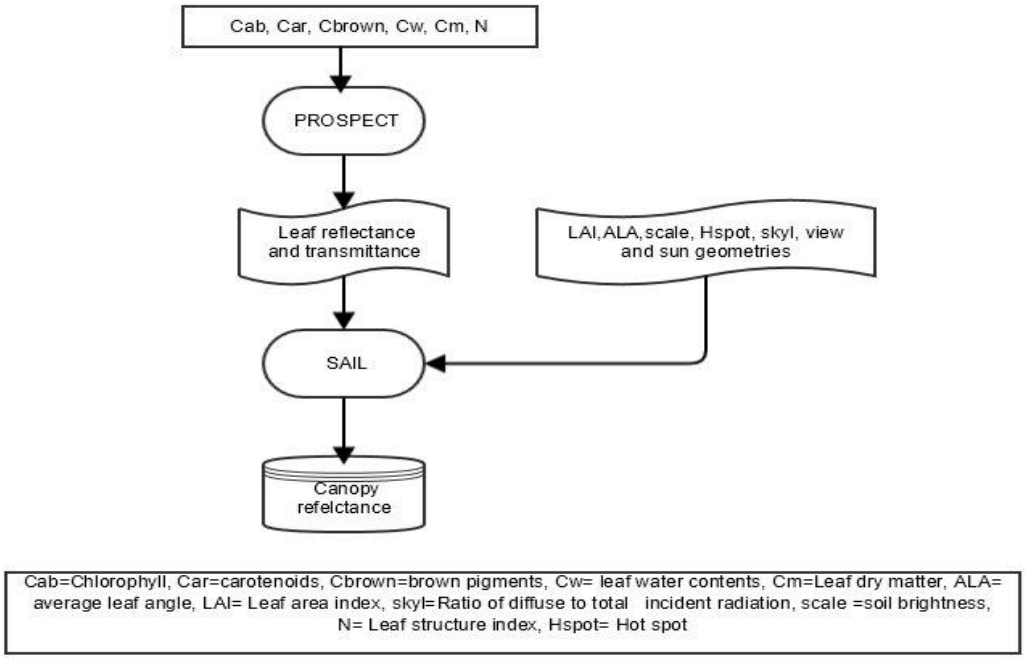

Figure 2.1. Illustration of radiative transfer models PROSPECT and SAIL**.**

The inversion is a technique in which canopy physical descriptors are estimated based on inputs of measured reflectance per pixel and the output of the PROSAIL. This has been done through minimization of merit cost function (Equation 2) e.g. optimization iteration approach (OPT) (Goel and Thompson 1984, Jacquemoud 1993; Jacquemoud et al. 1995; Meienberger 2010; LUT approaches (Weiss and Baret 1999; Weiss et al. 2000; Combal et al. 2002a; Fang and Liang, 2005; Scherf and Atzberger, 2006). Furthermore, non-parametric methods such as ANN and SVMs have been also used for inversion purposes (Weiss et al. 2000). However each of the above mentioned inversion approaches has its own advantages and drawbacks. For more on the advantages and disadvantages of inversion approaches can be found in Kimes el al. 2000 and Liang (2004). OPT is ruled out in this study due to intensive computations associated with the approach. LUT inversion is based on the generation of reflectance based on a combination of physical, biochemical and structural properties of the leaf of the given viewing and illumination geometry in table form (Weiss and Baret 1999; Weiss et al. 2000; Combal et al. 2002a; Fang and Liang, 2005; Scherf and

Atzberger, 2006). The best spectra are then selected as a solution through minimization of the cost function, root mean square error (RMSE) (Equation 2). RMSE is used to define the best fit between the measured spectra and the PROSAIL output in LUT.

Although LUT approach is time efficient, its robustness depends on data density (Weiss et al. 2000). In addition, the approach has a weakness of ill-posed problem (meaning that the inversion solution is not always unique as various combinations of canopy parameters can yield similar solution) (Combat et al. 2003). Fortunately, model parameterization adaptation based on prior information and regularization techniques has been proposed for the optimization of LUT inversion. For instance, the use of prior information (e.g. *in situ* data) as suggested by Combat et al. (2002) have proved to solve the problem. Also the use of multiple cases for the selection of inversion solution has also proved to increase robustness of the LUT inversion approach (Weiss et al. 2000; Darvishzadeh et al. 2011; Si et al. 2012).In addition Combat et al. 2002; Haboudane et al. 2008 and le Maire et al. 2008 demonstrated that the problem can be solved by using the modified cost function in the LUT inversion. Vohland and Jarmer, (2008) demonstrated the enhanced accuracy of LAI by coupling equivalent water thickness and dry matter content in a ratio of 4:1. However, LUT inversion is faced with discrepancies that exist on prior information and inverse strategy (Wang 2012). Consequently, machine learning such as ANN were investigated as an alternative to LUT (Weiss et al. 2000; Vuolo et al. 2010). Weiss et al. 2000 and Vuolo et al. 2010 have shown that ANN trained with generated LUT can solve the ill-posed problem of LUT. ANN is computational models in which connections of neurons in the human brain are simulated to establish the mapping function between the simulated reflectance and the corresponding biophysical variable of interest (Kimes et al. 2000).

The most used in remote sensing of vegetation is feed-forward multi-layer perceptron neural network (MLPNN) using error back propagation. During training of this network, the information moves forward from one layer to the next to compute the output. As it does so, the error is reduced between the actual and the desired output of the network in the gradient descent manner. This is done by propagating the

error back from output to input layer. In that way the weights of the connection and the biases are adjusted in order to minimize the mean square error of the prediction. Although training takes time, once done the ANN is very fast and efficient. It can also solve non-linear system problems without making assumptions as in more traditional statistical approaches. Both approaches showed good retrieval performances in estimating grass biophysical properties such as LAI (e.g. Table 2.3 (*b*)). From Table 2.3 it is evident that inversion of PROSAIL is a promising method for accurate estimates of LAI.

$$RMSE = \sqrt{\sum_{i=0}^{n} \frac{(Rmeasured - Rsimulated)^2}{n}}$$

(Equation 2)

However, the PROSAIL model was mostly applied to homogeneous canopies such as crops and forest (Table 2.3 (*a*)). There is little validation of PROSAIL in heterogeneous grassland e.g. Table 2.3(*b*). The studies by Si et al. (2012) and Darvishzadeh et al. (2008; 2011) are particularly relevant, accurately estimated heterogeneous grass LAI utilizing PROSAIL from MERIS and GER respectively. Darvishzadeh et al. 2011 obtained R^2 of 0.88, while, in the work of Si et al. (2012) reported accuracy for R^2 of 0.7. Although PROSAIL has shown success for estimating LAI in heterogeneous grassland of Italy (Darvishzadeh et al. 2008; 2011) and Netherlands (Si et al. 2012), it has not been validated for South African heterogeneous savannah. Thus, this study intended to assess the utility of this model for estimating LAI of SA grassland. The inversion of the models will be done using LUT and ANN approach, in which the materials and methods used are described in chapter 3 and chapter 4 of the thesis.

Table 2.2(*a*.) Reported studies of LAI estimation using univariate regression model.

METHOD USED	DATA USED	VEGETATION TYPE	RESULTS	REFERENCE
LAI-L-ATSAVI	Hyperspectral	Semi-arid mixed grassland	R^2 of 0.55	He et at 2006
LAI-NDVI REGRESSION	RapidEye	Corn & soybean	Sensitivity to LAI	Kross et al.2015
LAI-NDVI	Landsat 7/ETM+	Sugar cane, Pasture, corn, Eucalypt and Riparian forest	Standard error ranged from 0.42 to 0.87	Xavier & Vettorazzi (2004)

LAI-NDVI LAI-SR LAI-SAVI	Landsat TM	Grassland, Shrubland, Hardwood and Coniferous forest	NDVI-r2 of 0.74 SR- R^2 of 0.59 SAVI-r2 of 0.54	Turner et al. (1999)
LAI-MSAVI	QuickBird Images	Corn and Potato	MSAVI-LAI=rmse of 0.63 for corn RMSE of 0.79 for potato	Wu et al. 2007
LAI-NDVI REGRESSION	Landsat 5TM	Wheat, Corn	Corn-r2 of 0.88, 0.81 Wheat-r2 of 0.7	Wittamperuma et al.2012
SIMPLE LEAST LINEAR REGRESSION		Barley, wheat, Maize	NDVI-LAI overall RMS of 0.74	Houborg and Eva (2008)
LAI-NDVI	AWiFS	Wheat	R^2 of 0.79 RMSE of 0.52	Nigam et al. 2014
LAI-MCARI2 LAI-MTVI2	Hyperspectral	Soybean, Corn Wheat	Soybean-R^2=0.98,RMSE of 0.28 Corn=$R^2$of 0.89,RMSE of 0.46, Wheat-R^2 of 0.74, RMSE of 0.85	Haboudane et al.2004
LAI-VI Regression	GER data	*Asplenium nidus* *Halimium Umbellatum* *Schefflera Arboricola nora*	RVI-R^2 of 0.749 NDVI- R^2 of 0.748 PVI-R^2 of 0.741 TSAVI-R^2 of 0.681 SAVI2-R^2 0.78	Darvishzadeh et al. 2008
LAI and WDVI CLAIR MODEL	DEIMOS-1 Data	Agricultural crops	RMSE of 0.407 and R^2 of 0.88 for Italy RMSE of 0.86 and R^2 of 0.64 for the Austrian	Vuolo et al. 2013
LAI-PVI LAI-RVI LAI-NDVI	Spectroradiometer	Pearl millet grown in Indian arid zone	LAI-PVI-coeff.corr of 0.55 LAI-RVI-coeff of cor of 0.61 LAI-NDVI coeff-corr of 0.70	Boken and Chandra, 2012
LEAST SQUARE REGRESSION	Landsat Thematic Mapper (TM)	Crops	R^2 of 0.84	Bajwa et al. 2008
LAI-CIred-edge LAI- CIgreen LAI-MTCI	Hyperspectral	Maize and soybean	RMSE 0.577	Vina et al. 2011

Table 2.2 (*b*). Reported studies of LAI estimation using multivariate statistical methods.

METHOD USED	**DATA USED**	**VEGETATION TYPE**	**RESULTS**	**REFERENCE**
Bayesian network data fusion algorithm	MODIS	Winter wheat in	R^2 of 0.95 RMSE of 0.35	Qu et al. 2011
PLSR	GER data	Grassland	(SMLR) R^2 of 0.67 and (PLSR) of 0.87	Darvishzadeh et al. 2008
FUSION TECHNIQUE		Boreal forests	LAI-EVI-R^2 of 0.85	Hassan and Bourque, 2010

ANN	ASTER	Trees, shrubs, grass, corn and soybeans	R^2 of 0.71 SEE of 1.35	Jensen & Hardin, 2005
ANN	Landsat Thematic Mapper (TM)	Crops	R^2 of 0.91	Bajwa et al. 2008
ANN	Landsat ETM+	Corn and soybean	R^2 and RMSE of 0.63	Walthall et al. (2004)

Table 2.3 (*a*). Reported studies on estimation canopy biophysical variables by inversion of PROSAIL applied on crops and forest.

RS DATA	VEGETATION TYPE	METHOD USED	RESULTS	REFERENCE
Simulated canopy reflectance corresponding to TM	Simulated data	PCA	RMSE=0.137	Satapath and Dadhwal, 2004
Table 2.3(a)Applied on crops and forest				
Landsat TM & Landsat ETM+	Crops	LUT	R^2=0.97	González-Sanpedro et al.2007
MODIS	Rice	LUT	R^2 =0.69 RMSE =0.9	Nguyen et al. 2013
SPOT	Barley, wheat, maize	OPT	RMSD of 0.74	Houborg and Eva (2008)
MODIS & ETM+	Broad &Needle leaf canopies	LUT,ANN, PPR		Fang et al. 2004
L7 EMT+ & ASD		Genetic algorithm	R^2 =0.776 RMSE = 1.064	Fang et al. 2003
GER 1500	Potato	OPT	Retrieved realistic values of LAI	Casa and Jones 2004
MODIS	Wheat, maize, sunflower alfalfa crops	LUT & OPT	RMSE of 0.521	Tripathi et al. 2009
CHRIS	Alfalfa, maize, potatoes, sun-flower, onion, garlic, sugar beet and vineyard		RMSD of 0.79	Richter and Timmermans, 2009
AWiFS	Wheat	LUT	R^2 =0.91 RMSE of 0.34	Nigam et al. 2014
UAV	Maize	LUT	RMSE ~ 0.62	Duan et al. 2013
SPOT	Barley	ACRM	RMSE of 0.7	Houborg and Boeg 2007
DAIS	Polpar	OPT	confirms the operational potential of model inversion for LAI	Meroni et al. 2004
HyMap	Alfalfa	LUT	R^2 of 0.97	González-Sanpedro et al. (2008)
HyMap	Summer barley	LUT, OPT, ANN	OPT-R^2 of 0.94 LUT- R^2 of 0.94 ANN-R^2 of 0,7	Vohland et al. 2010
RapidEye	Crops	LUT &ANN	LUT $R^2$of 0.76 ANN $R^2$of 0.71	Vuolo et al. 2010
MERIS	Global domain	ANN	RMSE=0.47	Bacour et al.2006
ASD	Corn	LUT	R2=0.731, RMSE=0.663	Yang et al.2012
ASD FieldSpec II	Summer barley	OPT	R^2 = 0.90	Vohland et al. 2006
HyMap data	Summer barley	OPT	R^2 = 0.87	Vohland et al. 2006

Table 2.3 (b). Reported studies on estimation canopy biophysical variables by inversion of PROSAIL applied on heterogeneous grasslands.

RS DATA	VEGETATION TYPE	METHOD USED	RESULTS	REFERENCE
GER	Mediterranean grass	LUT	R^2 of 0.88	Darvishzadeh et al. 2008a
ASD	Grassland (Rhineland-Palatinate, Germany)	OPT	RMSE= 0.74, R^2 =0.778	Vohland and Jarmer 2008
MERIS	Grassland (Netherland)	LUT	R^2=0.70, RMSE=1.02, NRMSE=16%	Si et al. 2012

Chapter 3: Methodology and materials

3.1. Study area and Data collection

3.1.1 General description of study area.

The study was undertaken in Highveld grassland and savannahs of Mpumalanga province, east of South Africa (-24.92796 **S** 31.19515) **(**study area is shown in Figure 3.1). The Highveld grassland extends into the southwards to Bethal, Ermelo and west of Piet Retief (Mucina & Rutherford, 2006).

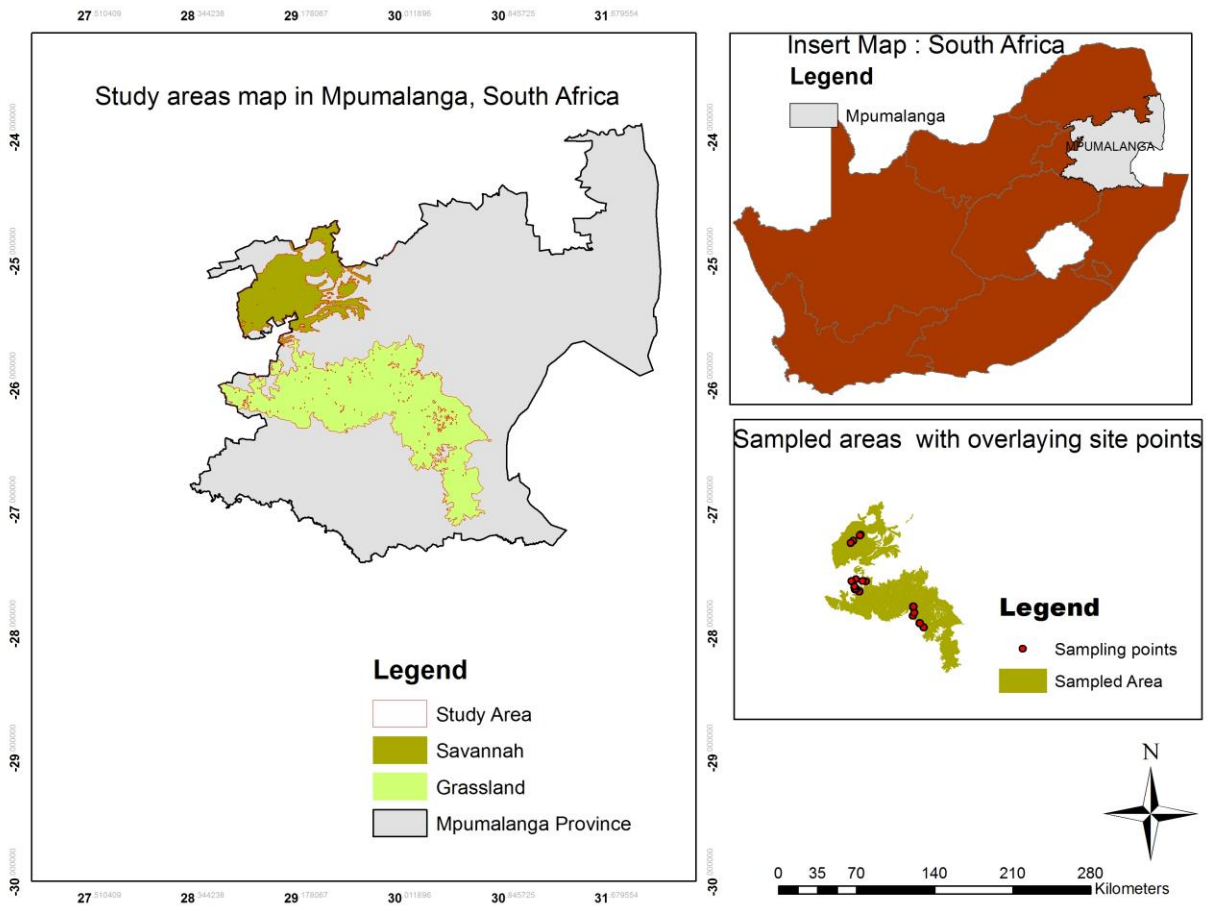

Figure 3.1. Study area map showing an insert of South African and sampled area, with projected coordinates.

The area is characterized by moderately undulating plains with low hills and pan depressions, topography extending southwards of Bethal, Ermelo and west of Piet Retief (Mucina et al. 2006). The topography is moderately undulating with altitude of 1520-1780m and as low as 1300 m (Mucina et al. 2006). The Eastern Highveld grassland covers land tenure transects ranging from statutory reserves (Nooitgedacht and Jericho Dam nature reserves) to privately-owned reserves (Holkranse, Kransbank and Morgenstond), cultivation, mining, plantations and state-owned communal areas. The climate is strongly seasonal - a summer rainfall with very dry winter.

The geology of the area is dominated by grass species reaching a height of ~2.1 m tall such as *Cymbopogon excavatus* and *Hyparrhenia hirta* and about 5% cover of herbaceous component averaging 50 cm tall with very few shrubs and trees. Dominant grass species are *Themeda triandra, Sporobolus africanus and Setaria sphacelata var. Sphacelata* whereas dominating herbaceous and shrub layers are *Setifera, Asparagus aethiopicus, Helichrysum aureonitens, Oxalis obliquifolia and Gnidia krau ssiana* (Mucina et al. 2006). In Figure 3.2 are photos representing an overview of the study site, taken during field work from 10-12 March, 2014. Rangelands in the privately-owned farms are grazed by cattle and goat. The communal rangelands support grazing of cattle and goats, which determine various grazing intensities.

Figure 3.2. An overview of study sites at Mpumalanga province (South Africa).

3.2 Data collection

3.2.1 *In situ* LAI collection

The collection of in situ LAI measurements was carried out from 10 to 12 March 2014. Due to accessibility restrictions, measurements were done mostly along the road, settlements and in open veld in the province. A purposive sample method was adopted and a total of 41 plots were sampled. The plots were distant by mostly 500m to 1000m; this was based on the homogeneity and accessibility of the area. The plot in each sampling point was randomly established in areas with homogeneous grass (Ramoelo et al. 2012). Each sample point was treated as a plot of greater than 100m x 100m, to account for a pixel size of the Landsat 8 image (30 m). The coordinates of the location of each point were recorded with the handheld Global Positioning System (GPS) (GARMIN GPSMAP 76, Garmin Ltd). LAI measurements were done as described in the paragraph below.

In each plot three subplots of 1m x 1m were randomly selected. In each subplot effective LAI measurements were done using the Plant Canopy Analyzer LAI- 2200 (LICOR Inc., Lincoln, NE, USA) (Licor (1992). This is one of the numerous commercially available optical instruments (Jonckheere et al.2004), which infer LAI from measurements of light transmission through a plant canopy. Field measurement of LAI were done under overcast sky conditions because it has been reported that Plant

Canopy Analyzer LAI- 2200 (LICOR Inc., Lincoln, NE, USA) (Licor (1992) tends to underestimate LAI under partial or direct sunlight conditions (Mazumdar 2011). The bias that could result from using LAI-2200 has been avoided by circumventing high level of light scattering off the leaf surface which could reach LAI -2200 sensor. This has been done by using transect oriented perpendicular to the solar azimuth during the measurement with LAI-2200.

To obtain the LAI measurement of the plot, an average LAI was calculated in each plot, based on the one above canopy measurement and five below-canopy measurements. Each LAI measurement comprises one above-canopy reading followed by below-canopy readings within two minutes to avoid atmospheric variation. Therefore, 3 measurements of LAI in a site were then averaged to provide an LAI value for the particular plot.

3.2.2. Remote sensed data collection and pre-processing.

3.2.2.1 Landsat 8 scenes collections

Table 3.1 depicts Landsat scenes used in this study and illumination geometries used for radiometric and surface reflectance calibrations. The satellite images are multispectral image Landsat 8 downloaded on-line from http://glovis.usgs.gov/. Landsat 8 is the eighth satellite in the Landsat program which joints Landsat 7 on-orbit. The image has three spectral channels added to the ones existing in previous Landsat. The sensor provides moderate-resolution imagery, from 15 meters to 100 meters of Earth's land surface which operate in the visible, near-infrared, short wave infrared (Table 3.2), and thermal infrared spectra. The Landsat 8 bands selected for this study are the six (2-7) bands showed in Table 3.2 and are centered at 480, 560, 655, 865, 1610, 2220 nm. In order to extract reflectance from these bands (Band 2- 7), the bands were preprocessed in which digital numbers are converted to surface reflectance. The pre-processing method followed here is described in the methodology section below.

Table 3.1. Landsat 8 scenes, date of acquisitions, illumination geometries used for calibration and parameterization of PROSAIL RT model.

LANDSAT_SCENE_ID	DATE_ACQUIRED	SUN_AZIMUTH	EARTH_SUN_DISTANCE	SUN_ELEVATION
LC81690782014089LGN00	2014-03-30	50.96401689	0.9986946	47.15288532
LC81700782014096LGN00	2014-04-06	47.78467206	1.0006798	45.52891094

Table 3.2. Used Landsat 8 bands descriptions (USGS 2014) (http://landsat.usgs.gov/band_designations_landsat_satellites.php).

SPECTRAL BAND	WAVELENGTH	RESOLUTION
Band 2 - Blue	0.450 - 0.515 µm	30 m
Band 3 - Green	0.525 - 0.600 µm	30 m
Band 4 - Red	0.630 - 0.680 µm	30 m
Band 5 - Near Infrared	0.845 - 0.885 µm	30 m
Band 6 - Short Wavelength Infrared	1.560 - 1.660 µm	30 m
Band 7 - Short Wavelength Infrared	2.100 - 2.300 µm	30 m

3.2.2.2 Pre-processing of Landsat Image

Radiometric calibration.

Pre-processing of the Landsat images comprised of first geo-coding of the images and then radiometric and atmospheric correction for the surface reflectance images. All downloaded Landsat 8 scenes were geo-coded by distributing ground control points over the Landsat imagery. Firstly the image was rectified using polynomial transformation with an error lower than one as was done in Gonzalez-Sanpedro et al. 2009, followed by resampling at 30m spatial resolution using cubic convolution method. The radiometric calibration was done by calculating the at-sensor radiance using Equation. 3 given by: (https://landsat.usgs.gov/Landsat8_Using_Product.php). Table 3.3 depicts band-specific multiplicative

rescaling factor and band-specific additive rescaling used. This was conducted using band math function on a software package called ENVI 4.7 (Environment for Visualizing Images). ENVI 4.7 was chosen because it has numerous utilities for the visualization, analysis and presentation of the digital imagery.

$$L\lambda = M_L * Q_{cal} + A_L \quad \text{(Equation 3)}$$

Where: M_L and A_L are Band-specific multiplicative rescaling factor and band-specific additive rescaling factor respectively. Both are from Landsat 8 metadata file, M_L is presented as RADIANCE_MULT_BAND_x, and A_L as RADIANCE_ADD_BAND_x and x is the band number, whereas Qcal is a quantized and calibrated standard product pixel values (DN).

The above mentioned expression was computed for each of the seven bands. Then, all bands were overlaid in one file through stacking using ENVI 4.7. During the process, bands were named accordingly and band centers were included and then converted to reflectance as explained below.

Table 3.3. Landsat 8 band-specific additive and multiplicative rescaling factor used for radiometric calibration (http://glovis.usgs.gov)

Landsat 8 scenes used	Band-specific-additive rescaling factor	Band-specific-multiplicative rescaling factor
LC81700782014096LGN00"	BAND_1 = 1.2539E-02	BAND_1 = -62.69351
	BAND_2 = 1.2840E-02	BAND_2 = -64.19892
	BAND_3 = 1.1832E-02	BAND_3 = -59.15875
	BAND_4 = 9.9772E-03	BAND_4 = -49.88599
	BAND_5 = 6.1055E-03	BAND_5 = -30.52774
	BAND_6 = 1.5184E-03	BAND_6 = -7.59197
	BAND_7 = 5.1178E-04	BAND_7 = -2.55890

LC81690782014089LGN00	BAND_1 = 1.2589E-02	BAND_1 = -62.94301
	BAND_2 = 1.2891E-02	BAND_2 = -64.45441
	BAND_3 = 1.1879E-02	BAND_3 = -59.39418
	BAND_4 = 1.0017E-02	BAND_4 = -50.08452
	BAND_5 = 6.1298E-03	BAND_5 = -30.64923
	BAND_6 = 1.5244E-03	BAND_6 = -7.62218
	BAND_7 = 5.1382E-04	BAND_7 = -2.56908

Conversion radiance to surface reflectance.

In order to use Landsat 8 for prediction of the LAI, the reflectance of the image need to be extracted and used for inversion of the PROSAIL model. Thus, Landsat surface radiances were converted into the reflectance, the ratio of radiance to irradiance. For this purpose surface reflectance was computed using Quick Atmospheric Correction methods also available in ENVI 4.7©. Since Landsat-8 is a new sensor and has not been added to the Quick Atmospheric Correction list of sensors for ENVI 4.7, an 'Unknown ' sensor type was chosen. Then spectral reflectance corresponding to the ground points where LAI was measured in the field were extracted from the image using the spectral extraction function in ENVI 4.7 software. To eliminate the inclusion of pixel outside the plot the grass spectral was collected using 7 by 7 pixel window (Cho et al. 2008). The collected spectral were then averaged and then used during for LUT and ANN inversion and also for computation of vegetation indices used in the study as described in the following chapter.

Chapter 4: Leaf area index derivation

In this study LAI was estimated using physical based PROSAILH radiative transfer models inverted on Landsat 8 remote sensing data. The model was inverted using look-up table and artificial neural network algorithms. Furthermore, we assessed the accuracy of the RTM model in comparison with empirical methods in estimating LAI. The methodology followed is depicted in Figure 4.1 below.

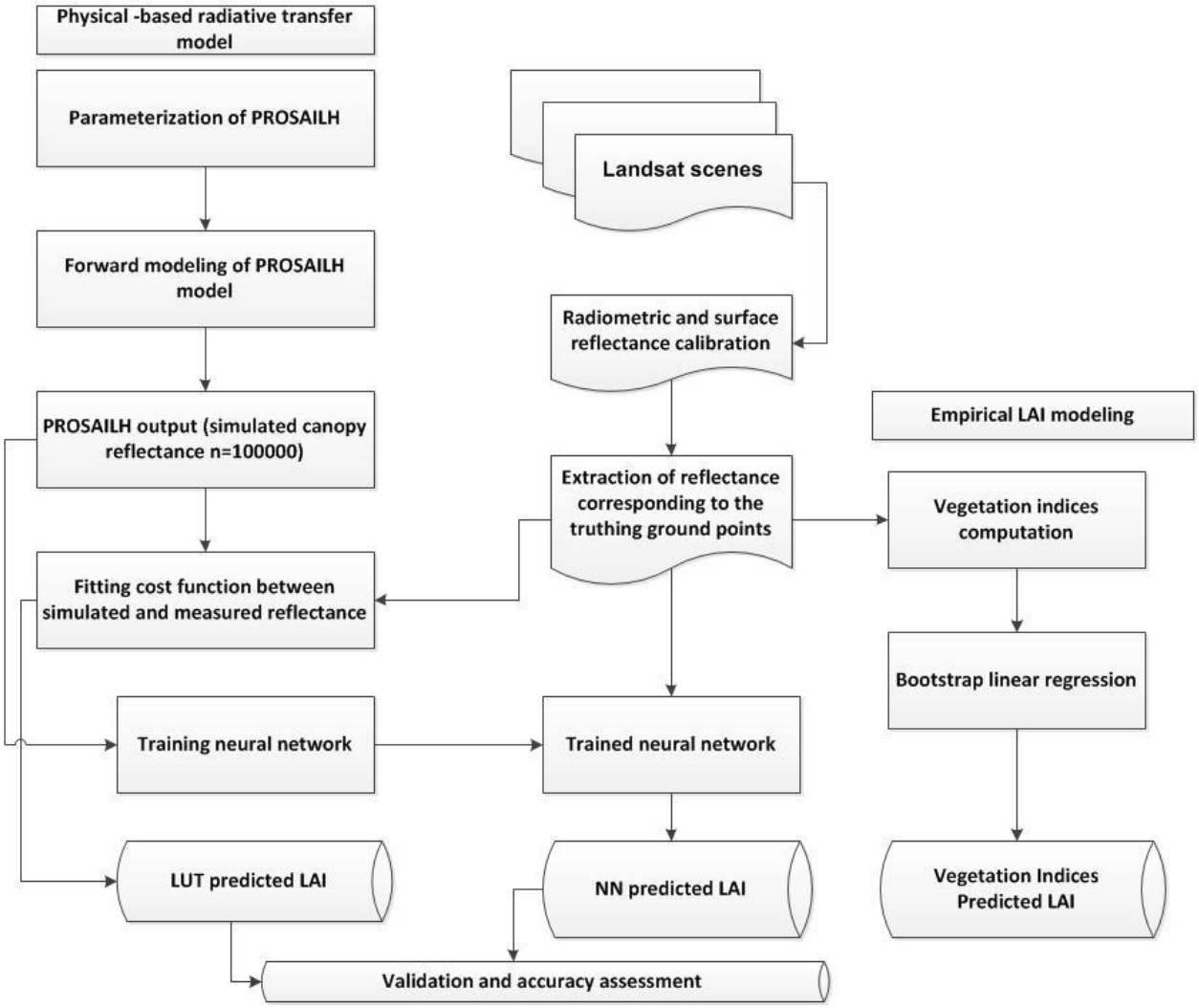

Figure 4.1. The conceptual outline of the study.

4.1 LAI derivation using the PROSAIL model.

MATLAB version of PROSAIL (PROSPECT+SAIL=PROSAIL, obtained from http://teledetection.ipgp.jussieu.fr/prosail/) was used for the estimation of LAI. This model uses chemical concentration's specific absorption coefficients and structural properties of the leaf of the given viewing and illumination geometry in the forward mode to simulate canopy spectral reflectance at 5 nm interval over 400–2500 nm (Figure 4.2). For the simulation of Landsat 8 spectral band sensor spectral resampling was done in the model. The ENVI version 4.7 software used for resampling did not have Landsat 8 filter function; therefore unknown filter function was used instead to give six bands spectra. As a result the model matched the Landsat 8 sensor characteristics and simulated leaf canopy reflectance corresponding exactly to the wavelength used by the Landsat 8 sensor (Figure 4.3). The six bands are centered around 484, 561, 654, 865, 1609, 2201 nm.

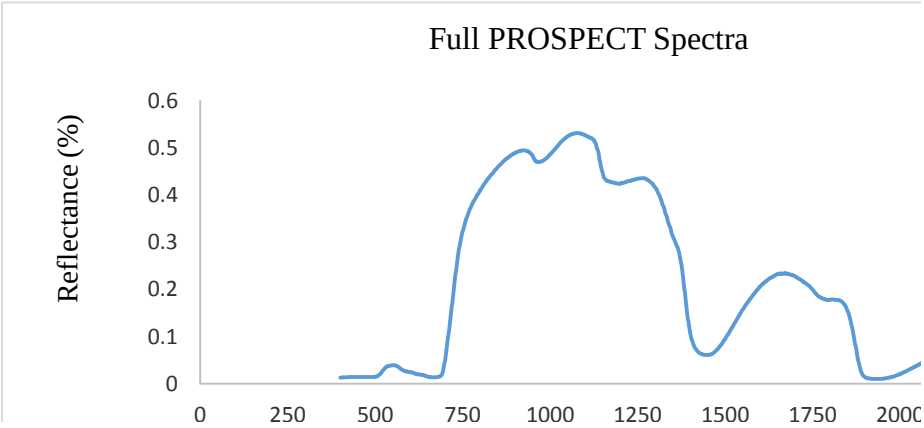

Figure 4.2. Leaf reflectance simulated over solar spectrum from 400 nm to 2500 nm.

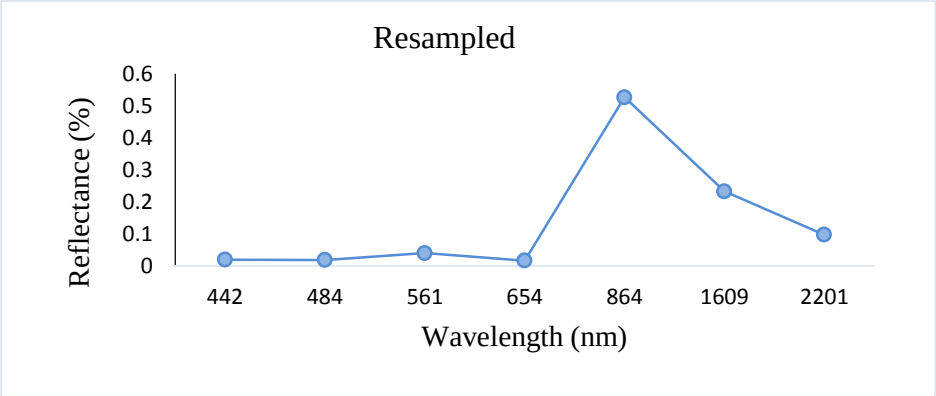

Figure 4.3. Resampled PROSAIL canopy reflectance to match Landsat 8 sensor.

The PROSAIL was used to simulate a set of spectra for specific model inputs (parameters). The inputs were parameterized based on minimum and maximum limits of the respective parameters as shown in Table 7. Most parameters were based on information retrieved from past studies conducted particularly on electrophile architectures vegetation such as grass (e.g. Darvishzadeh et al. 2008; Vohland & Jarmer 2008; and Si et al. 2012). However, minimum and maximum bounds of the LAI were based on the prior knowledge from the field data collection (Combal et al. 2003). Soil spectral was extracted from the bare site next to the field site on the image using ENVI 4.7 software, and then averaged. Hot spot and scale were selected similarly in agreement with Darvishzadeh et al. (2008) and Si et al. (2012). The geometrical parameters (per pixel sun zenith angle, sensor viewing angle and relative azimuth angle) were collected from the metadata provided with each Landsat 8 image. Due to small effect diffuse incoming solar radiation called ratio of diffuse to total incident radiation (*skyl*), have on canopy reflectance (Clevers and Verhoef 1991), a fixed value of 0.1 across all wavelengths has been used, as in many similar studies (Schlerf and Atzberger 2006; Si et al. 2012; Darvishzadeh et al. 2008). From these parameter canopy reflectance were simulated and stored in the LUT, then used for inversion as described in the following sections.

Table 4.1. Specification of parameter ranges and distributions for SAIL+PROSPECT reflectance modelling. The abbreviations and units of the parameter used are shown in symbol and units columns. The minimum and maximum ranges of the parameters are also shown in ranges columns.

PARAMETERS	SYMBOL	UNITS	RANGES (Min-Max)
Leaf structure index*	N	dimensionless	1.5-1.9
Leaf chlorophyll content*	Cab	μgcm^{-2}	15-55
Leaf dry matter content*	Cm	gcm^{-2}	0.0025 - 0.005
Carotenoids content *	Car	$\mu\ g/cm^2$	0-25
Brown pigments content*	Cbrown	No units	0-1
Leaf water content[a]	Cw	gcm^{-2}	0.01- 0.02
Leaf area index[b]	LAI	m^2m^2	1-5
Average leaf angle *	ALA	deg	20-70
Hot spot parameter *	hot	$m\ m^{-1}$	0.05-0.10
Ratio of diffuse to total incident radiation	skyl	%	0.1[e]
Soil brightness	scale	No dimension	0.5-1.5
Sun zenith angle [c]	φv	deg	Fixed per pixel
View zenith angle [c]	φs	deg	Fixed per pixel
View zenith angle [c]	φ	deg	Fixed per pixel

* Range were constraint based on past studies, [a] Coupled with equivalent water thickness in the ratio 4:1,
[b] Range in the field level: 1-5, [c] fixed based on information from used Landsat 8 scenes metadata.

4.2.1. Grass LAI estimation based on LUT inversion.

Weiss et al. (2000), states that the larger the LUT, the higher the chances of retrieving accurate parameter. Therefore various iterations in the interval of 5000 were tested (results are shown in Appendix A). After testing various alterations and 100,000 iterations, it was possible to estimate LAI with slightly higher accuracy. LUT with simulated spectra was generated with PROSAIL by using randomly distributed

minimum and maximum bounds of the parameters spaced using uniform random sampling according to Equation 4. For estimation of LAI, LUT was inverted by finding which spectrum from the Look-Up Table minimizes the expression depicted in Equation 5 (RMSE). RMSE signified the sum of square differences between Landsat 8 pixel band reflectances and model simulated canopy reflectance. For the selection of the optimal solution, multiple best spectra and computation of the median and mean of their corresponding parameters were used. This was based on the Weiss et al 2000 findings that one best spectrum does not guarantee best solution. The LAI values belonging to the best spectra were then chosen and their mean and median was calculated. The overall time taken for inversion was 288.23 seconds in MATLAB version R2009a on 64-bit Windows 8 platform. The performance of the model was then evaluated using accuracy measures described in section 4.4.

$$F(n) = a-(b-a)* \text{rand}(n) \qquad \text{(Equation 4.)}$$

$$RMSE = \sqrt{\sum_{i=0}^{n} \frac{(Rmeasured - Rsimulated)^2}{n}} \qquad \text{(Equation 5.)}$$

Where *Rmeasured* the LAI is measured in the field, *Rsimulated* is the LAI estimated from the PROSAIL model, and comprises the number of readings as measured in the field. Where F is variable, **a** and **b** are maximum and minimum limits of the variables, respectively, whereas, n is the number of iterations used for the creation of LUT.

4.2.2. Grass LAI estimation based on artificial neural network inversion.

The performance of the ANN was also tested for the accurate estimation of LAI in South African savannahs. For the training, MATLAB feed-forward MLPNN using error back propagation was utilized. The use of MLPNN network was based on the literature review because it is by far the most used network in remote sensing. For training purposes, synthetic data generated for the LUT inversion was used.

Due to lack of proven criteria for determining the adequate architecture, it was necessary to experiment with various ANN architectures. For that purpose, training validations and tests were done with various

structures and selected best network. This was done by training the network with learning rates of 0.01, 0.05, 0.5 and 1 respectively. To find optimal hidden layers, the number of neurons in the hidden layer was increased to a smaller value of error and the higher value of R^2 was found. For that purpose the network was trained with various numbers of hidden units varied from 5 to 50. Hidden units that gave satisfactory results were taken as optimal hidden units. The activation function is also crucial during training for transformation of activation level of a neuron into an output. Therefore the appropriate activation function for optimal network was also investigated. For neurons in the hidden layers, hyperbolic tangent function (tansig) was used and logsig and purelin functions were investigated for output neurons.

The over-fitting problem of the ANN was prevented by early stopping criteria. The data was divided into three subsets in which the first subset of 70% of the data was used in the training phase, 15% in the testing phase and the remaining 15% for validation. The validation subset was used to stop training when the network begins to over-fit the data. Other parameters used include maximum validation failures of ten (10), training goals include MSE of 0.001, a minimum gradient of 10^{-8}, and a maximum epoch of 2000. The training stopped when any one of these training goals was met, but was stopped when maximum validation failure was reached. The network performance was measured by observing MSE and R^2 values during training. From the results, the three best networks were selected and are shown as ANN-14, ANN-15 and ANN-16 in the results section.

4.3 LAI derivation using empirical models.

The in situ field measured LAI (LAI-2200) estimates were correlated with various vegetation indices derived from Landsat 8 scenes. Table 4.2 shows vegetation indices (VIs) used in this study and their respective equations. The VIs indices used include ratio based VIs, atmospherically resilient vegetation indices and soil- adjusted VIs. Vegetation indices were computed from respective Landsat 8 bands as shown in Table 4.2, followed by extraction of VI corresponding to the sampled points. Linear regression was developed to find the best fit between field measure LAI and each of the spectral indices. Vegetation

indices were used as independent variables to predict dependent variable LAI. The regression was done as explained in subsection 4.3.2 below.

Table 4.2. Outline of VIs used for the estimation of grass LAI. Formulation is based on Landsat 8 imagery bands.

Name of VI used	Acronym	Equation based on Landsat 8 bands (B5(NIR), B4 (Red band), B3(Green band), B2 (Blue band)	References
Difference vegetation index	DVI	B5 – B4	Tucker, 1979
Normalized Difference Vegetation Index	NDVI	(B5 – B4) / (B5 + B4)	Rouse, 1973
Green index	GI	GI=(B5/B3)-1	Gitelson et al. 2003
Normalized green	NG	B3 / (B5 + B4 + B3)	Sripada et al. 2006)
Normalized red	NR	B5/ (B5+ B4+ B3)	Sripada et al. 2006
Normalized near infrared	NNIR	B5 / (B5 + B4 + B3)	Sripada et al. 2006
Infrared percentage vegetation index	IPVI	B5/ (B5 + B4)	Crippen, 1990
Structural Independent pigment index	SIPI	B5-B2/B5-B4	Penuelas et al. 1995
Ratio Vegetation Index (also known as the Simple Ratio)	RVI	B5 / B4	Birth and McVey, 1968
Green infrared percentage vegetation index	GIPVI	B5 / (B5+ B3)	Crippen, 1990
Enhance vegetation index	EVI	[(B5– B4) / (B5 + C1*B4 – C2*B2 + L)]	Liu and Huete, 1995
Green optimized soil adjusted vegetation index	GOSAVI	[(B5 – B3) / (B5 + B3 +L)] * (1 + L)	Cao et al. (2013), modified from Rondeaux et al. (1996)
SAVI	SAVI	[(B5– B4) / (B5+ B4 +L)] * (1 + L)	Huete, 1988, Rondeaux et al. 1996
Optimized soil adjusted vegetation index	OSAVI	(B5-B4)(1+0.16)/(B5+B4+0.16)	(Qi et al. 1994)
Green soil adjusted vegetation index	GSAVI	[(B5 – B3) / (B5 + B3 +L)] * (1 + L), where L = 0.5	(Gilabert et al. 2002)
Green atmospherically resilient index	GARI	B5 – [B3 – (B2 – B4)] / B5 [B3 – (B2 – B5)]	Gitelson et al. 2002

L= is a correction factor which ranges from 0 for very high vegetation cover to 1 for very low vegetation cover. The value of L used was 0.5 as was found to be optimal by Huete (1998). For OSAVI, L is a correction factor that equals 0.16.For EVI, L was set to 1.

4.3.1 Extraction of vegetation indices.

For the calculations of VIs, band math function on ENVI 4.7 (Environment for Visualizing Images) was used using equations as shown in Table 4.2. The VI values were established by noting VI values at the points corresponding to the ground truthing points where field measurements of LAI were made. This was done by averaging the VI values of the nearest pixels to the Universal Transverse Mercator (UTM) coordinates of the ground truth sites. Appendix B presents computed VIs values at the points corresponding to the ground truth points where LAI was measured. Then the relationship that exists between ground-based measures LAI and each of the VI was analyzed using the bootstrap and linear regression.

4.3.2 Regression of LAI on used vegetation indices.

To find the correlation between calculated vegetation indices and LAI a bootstrap cross-validation approach was adopted in this study using R programming language version 3.1.2 (2014-10-31) -- "Pumpkin Helmet. Bootstrap was suitable because of a limited number of samples the study had. The technique iteratively (100 iterations were used) used to split the data into calibration and validation data set. For regression, linear model was fit to the calibration data set between field measured LAI and vegetation index. Then the model was applied to predict the output values of the validation data set. Subsequently, the RMSE and coefficient of determination (R^2) were calculated for both calibration and validation data set, then recorded together with slope and intercept of the straight line obtained. This was done before the start of each iteration. The RMSE and R^2 obtained from each iteration were then averaged and noted as an accurate measure of the LAI-VIs relationship.

4.4 Accuracy assessment.

The efficiency of models is evaluated by both RMSE and coefficient of determination (R^2) between modelled and measured LAI. R^2 is given in Equation 6 and used to assess the proportion of the variance explained by the regression model. RMSE (Equation 8) measure the error of absolute fit between

measured and the modelled LAI data, where RMSE values close to zero signify absolute fit. Because RMSE has the same units as the data (LAI), it is advantageous as the deviation is directly comparable to the value of the parameter (de Jong, 2005).Whereas, the bias is used to evaluate the performance of the approach by measuring how modelled values differ from the measured values, and indicates whether there is under- or overestimation. All 41 ground truthing points were used for the evaluation.

$$r^2 = \left[\frac{\sum(x.y) - \sum x.\sum y}{\sqrt{\{n\sum(x^2) - (\sum x)^2\}.\{n\sum(y^2) - (\sum y)^2\}}}\right]^2 \quad \text{(Equation .6)}$$

$$\text{Bias} = \sum(x-y)/n \quad \text{(Equation. 7)}$$

$$RMSE = \sqrt{\frac{\sum_n^i (x-y)^2}{n}} \quad \text{(Equation. 8)}$$

X or x is an individual measured reflection data and Y or y is an individual modelled reflection data and *n* a number of measurements values. For interpretation of bias, low values indicate no deviation between measured and modelled value, while high values indicate high level of inaccuracy. The negative value shows underestimations while positive values are a sign of overestimation.

Chapter 5: Results

5.1 Accuracy of RTM (PROSAIL) in retrieving grass LAI from Landsat 8 imagery.

Generally, as depicted in Table 5.1 and Figure 5.1 inversions of PROSAIL radiative transfer on Landsat 8 imagery yielded accurate estimates of LAI values in the savannah grass. The results of inversion of the PROSAIL radiative transfer model for the derivation of grass LAI were divided into two groups: (i) LUT-based inversion algorithm (ii) ANN based inversion algorithm. Amongst the two algorithms ANN inversion algorithm yielded the highest accuracy estimates of LAI values in the savannah grass with RMSE of 0.138) and LAI variance of 87, 7%. In contrast, LUT inversion algorithm yielded an intermediate accuracy (RMSE= 0.265) and LAI variance of 50%. However, based on bias values depicted in Table 5.1 there is a slight overestimation in both techniques. LUT overestimated LAI retrieval with a bias of 0.028, while ANN shows a bias of 0.039 which is slightly higher than that of LUT. However, both models yielded low bias, thus there is reasonable prediction accuracy. Overall the accuracy of retrieved LAI was demonstrated by ANN inversion with high correlation and small predictive error.

Table 5.1. Best fit models for the correlation relationships between PROSAILH estimated LAI and field measured Leaf Area Index.[a] Represent observed accuracy between measured LAI and PROSAILH estimated LAI inverted with LUT. [b] Represent observed accuracy between measured LAI and PROSAILH estimated LAI inverted with ANN algorithm.

Model	**R^2**	**RMSE**	**Bias**
LUT[a]	0.501	0.265	0.028
ANN14[b]	0.877	0.138	0.039

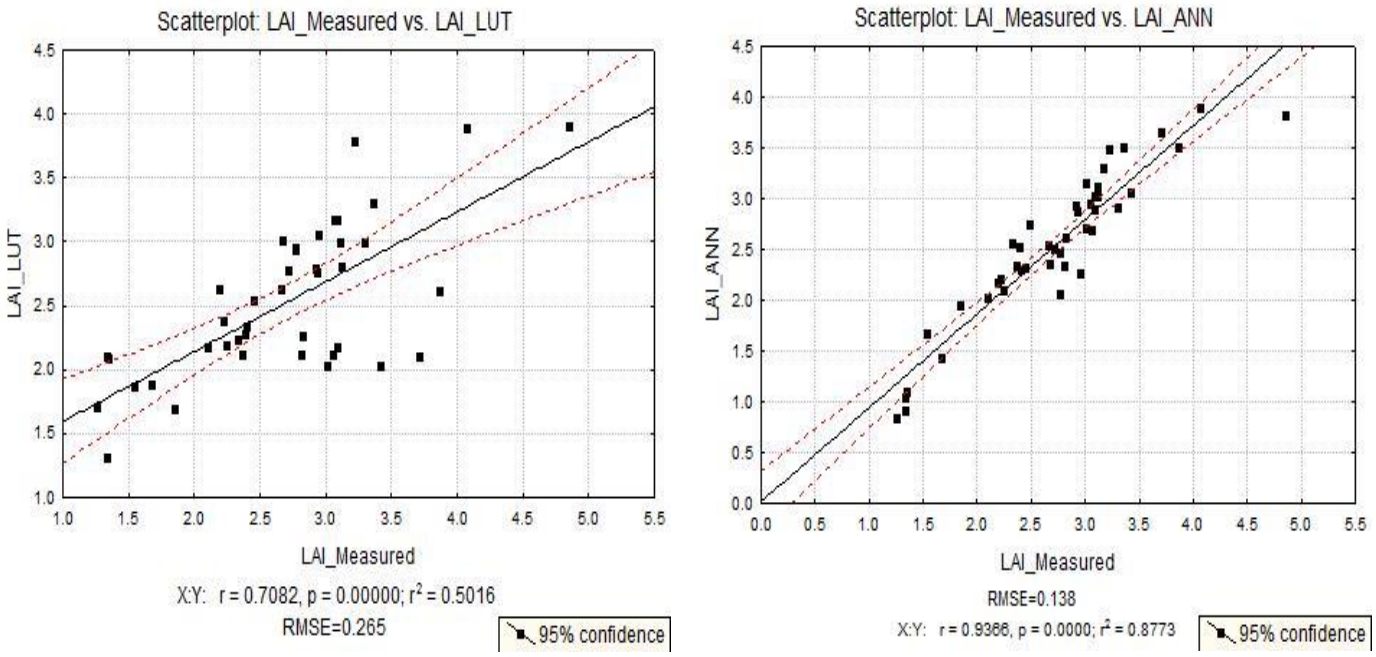

Figure 5.1. Relationship between PROSAIL estimated LAI and field measured LAI (m^2m^{-2}) (a) LUT and (b) ANN. R^2 =coefficient of determination and RMSE= root mean square error.

5.1.1 Optimization of LUT based inversion.

Because LUT tend to suffer from ill-posed problem, some measures were carried out during configuration of LUT in order to minimize such problems. For instance, for the selection of optimal solution, distribution of multiple best spectra and computation of their means and median was used and the results are depicted in Table 5.2 (a). From Table 5.2(a), the best 50 cases provided intermediate accuracy than one best case, with measured and the estimated output RMSE value of 0.363. The one best case yielded the highest RMSE of 0.429 and lowest R^2 (0.3543) which show poor accuracy contrary to other cases. On the other hand, the 100 best cases were the best amongst three cases with the lowest RMSE (0.265) and the highest R^2 value of 0.501 which indicate the reasonable accuracy between measured and the estimated LAI. Thus based on the lowest RMSE and highest R^2, the best 100 cases were selected as the LUT

inversion solution. Another thing that was taken into consideration in LUT inversion was the density of the LUT, as mentioned by Weiss et al. (2000) the larger the LUT the higher the chances of retrieving accurate parameter. In this study the accuracy of the LUT also depended on the number of iterations. The RMSE and R^2 obtained from various LUT iterations are presented in Table 5.3 and detailed in Appendix B. Results showed that, the RMSE decreased with increasing number of iterations. The minimum RMSE (0.501) was achieved when 100,000 iterations were used. The performance of optimal LUT for estimating grass LAI in this study site is presented in Table 5.2 (a). The R^2, RMSE, and bias of an optimal LUT were 0.501, 0.265, and 0.028, respectively.

5.1.2 Optimization of ANN based inversion.

Regarding the solution of the ANN inversion, the first thing was to determine the optimal network based on defined function with differentiated neurons in the hidden layer. This was done by using various learning rates and training functions and the best network was chosen as shown in Table 5.2 (b) and more detailed results are illustrated in Appendix C. From the results depicted in Appendix C the most optimal models based on the small error observed from validation and testing sets were found to be ANN14, ANN15, and ANN16 (Table 5.2 (b)). As shown in Table 5.2 (b), model ANN14 model was able to explain 87 % of variability of LAI and resulted in a fairly low RMSE of 0.138. Therefore based on R^2 and RMSE, model ANN-14 is the best model for estimation of LAI as compared to others. Thus, it was chosen as the solution to the ANN inversion and compared to LUT inversion solution as shown in Figure 5.1.

Table 5.2. Statistical indices of grass LAI, (a) results of LUT from using various number of cases in the solution, (b) three best models obtained from optimization process of ANN.

(a) LUT inversion				
Nr of case used to find solution	**Statistical parameters**	**R^2**	**RMSE**	**Bias**
1 best solution	N/A	0.3543	0.429	0.5
best 50 solution	mean	0.4802	0.398	0.1
	Median	0.4826	0.363	0.21
best 100 solution [a]	**mean**	**0.5016**	**0.265**	**0.028**
	Median	**0.5016**	**0.265**	**0.028**
(b) ANN inversion				
Model	**Net arch[c]**	**R^2**	**RMSE**	**Bias**
ANN-14[b]	**6-20-1**	**0.873**	**0.138**	**0.039**
ANN-15	6-25-1	0.7818	0.1642	0.29
ANN-16	6-30-1	0.7698	0.175	0.32

RMSE=root mean square error, R^2= coefficient of determination, Net-arch[c]= network architecture

[a] LUT solution, [b] ANN solution.

Table 5.3. Coefficients of determination (R^2) and Root mean square error (RMSE) accuracy assessment between measured LAI and modelled LAI based on different number of iteration. RMSE= root mean square error, R^2 = coefficient of determination, Nr of iterations=number of iterations used for the creation of LUT.

Nr of iterations	**RMSE**	**R^2**
5000	0.85940	0.077
10000	0.79795	0.118
15000	0.7991	0.040
20000	0.7671	0.097
25000	0.7473	0.165
30000	0.7482	0.160
35000	0.7246	0.050
40000	0.7221	0.304
45000	0.7045	0.204
50000	0.6138	0.337
100000	0.265	0.501

5.2 Performance of empirical modelling for estimation of grass LAI using Landsat 8 data.

The results of semi empirical approach are presented in Table 5.4 which includes the relationship between the vegetation indices and LAI for calibration and validation set. It should be noted that the relationship between LAI and vegetation indices reported in this study is based on the linear relation (Table 5.4, figure 5.2 and 5.3). From three categories of indices used, the best fit was observed from ratio based indices, followed by soil adjusted indices (SAVI, GOSAVI, OSAVI, GSAVI2 and GSAVI). The least fit was observed with atmospherically resilience indices (GARI and VARIgreen). From the ratio based group, GIPVI, GI and NDVI (Figure 5.4 and Table 5.4) were the best amongst others with RMSE of 0.308, 0.306, 0.319 and 0.287, 0.268 and 0.327 for calibration and validation, respectively. Their scatter plots are depicted in Figure 10 below. On the other hand GOSAVI showed best correlation with LAI amongst soil adjusted indices with RMSE of 0.339 and 0.347 for calibration and validation, respectively. The least performer is GARI with observed RMSE of 1.401(Table 5.4, Figure 5.2 and Figure 5.3). Generally, the results regularly demonstrated reasonable accuracy of ratio based indices using green band (GIPVI, GI, NG, NR and NNIR) and NDVI. This could be due to high reflectance of heterogeneous grass on green bands as reported by He et al. (2006). The study reported a much higher reflectance in the green reflection region and weaker in the near infrared (NIR) region of heterogeneous grass when compared with the typical vegetation spectral curve.

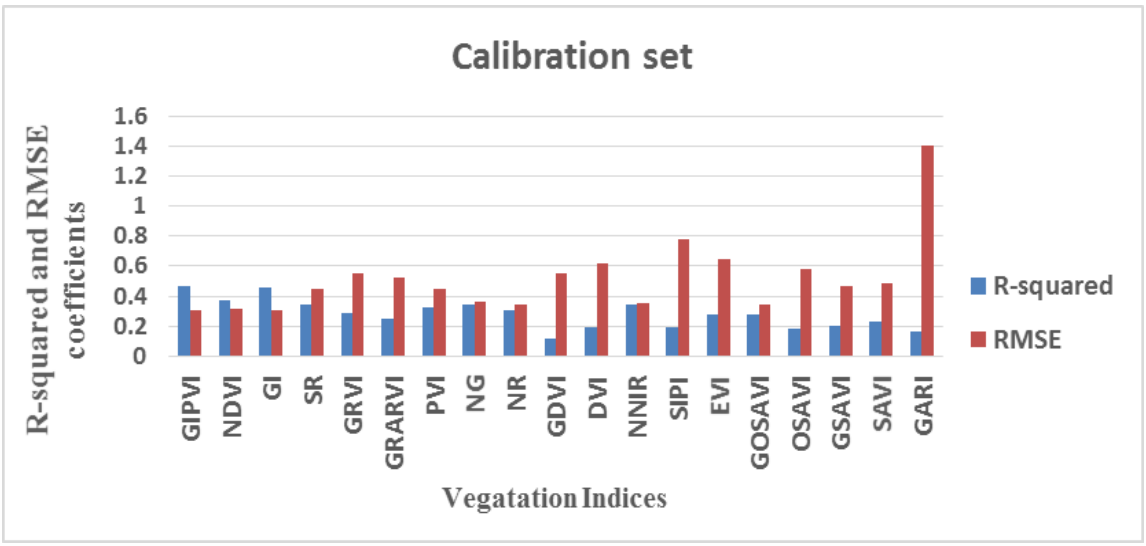

Figure 5.2. Observed coefficient of determination (R^2) and Root Mean Square Error (RMSE) for the fitted function correlating LAI with Landsat 8 derived vegetation indices for calibration set.

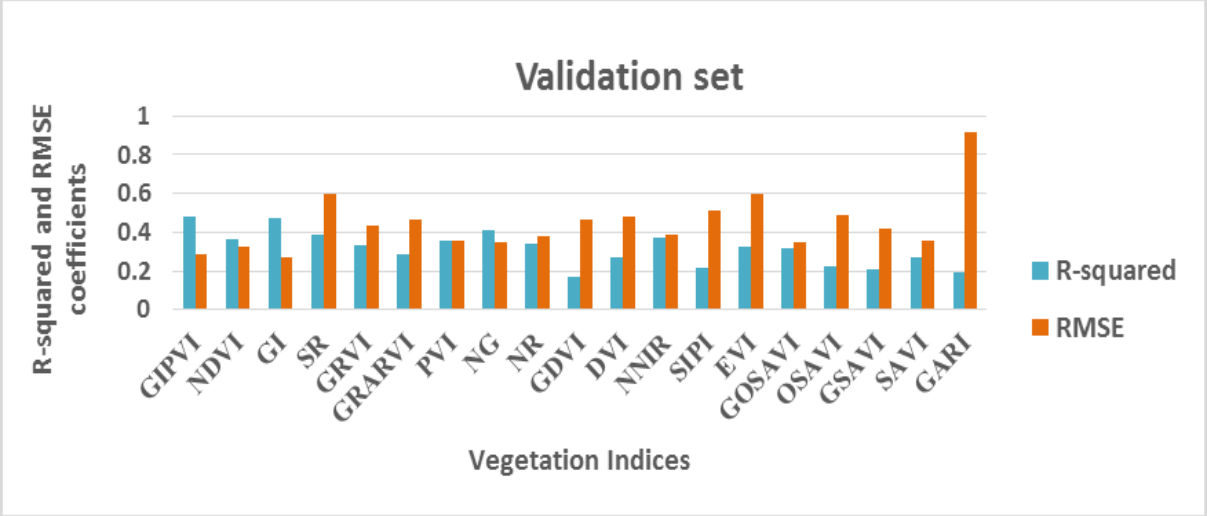

Figure 5.3. Observed coefficient of determination (R^2) and Root Mean Square Error (RMSE) for the fitted function correlating LAI with Landsat 8 derived vegetation indices for validation set.

Table 5.4. Best performed functions of the correlation relationships between vegetation indices and in situ field LAI obtained from calibration, N=30 and Validation (N=11).

Vegetation Indices	Calibration results (N=30)		Validation results (N=11)	
	R^2	RMSE	R^2	RMSE
GIPVI	0.465	0.308	0.484	0.287
NDVI	0.3765	0.319	0.363	0.327
GI	0.460	0.306	0.476	0.268
SR	0.348	0.447	0.385	0.598
GRVI	0.289	0.552	0.333	0.433
GRARVI	0.246	0.528	0.286	0.468
PVI	0.327	0.447	0.359	0.352
NG	0.346	0.362	0.411	0.351
NR	0.303	0.341	0.341	0.380
GDVI	0.120	0.552	0.172	0.464
DVI	0.194	0.621	0.272	0.484
NNIR	0.346	0.352	0.369	0.385
SIPI	0.1921	0.782	0.216	0.511
EVI	0.276	0.647	0.328	0.601
GOSAVI	0.277	0.339	0.320	0.347
OSAVI	0.181	0.576	0.227	0.488
GSAVI	0.203	0.462	0.211	0.422
SAVI	0.228	0.481	0.272	0.359
GARI	0.161	1.401	0.190	0.913

RMSE= root mean squared error of the LAI estimations. R^2= coefficient of determination. GIPVI= Green Infrared Percentage Vegetation Index ,NDVI= Normalized Difference Vegetation Index, GI=Green Index, NG= Normalized Green, NR= Normalized Red, SR= Ratio Vegetation Index (also known as the Simple Ratio), EVI= Enhance Vegetation Index, GSAVI= Green Soil Adjusted Vegetation Index, SAVI= Soil Adjusted Vegetation Index, OSAVI= Optimized Soil Adjusted Vegetation Index, GOSAVI= Green Optimized Soil Adjusted Vegetation Index , DVI= Difference Vegetation Index , GARI= Green Atmospherically Resilient Index , SIPI= , NNIR= Normalized Near Infrared , GI=Green Index, GRVI= Green-Red Vegetation Index, IPVI=Infrared Percentage Vegetation Index.

(a) **(b)**

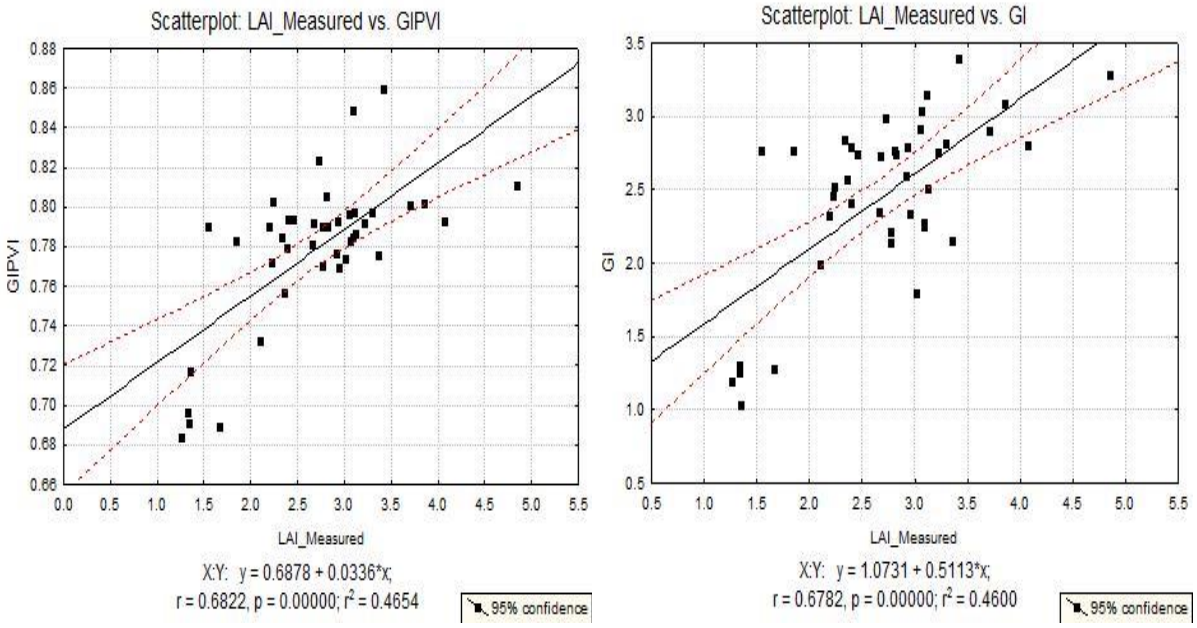

(c)

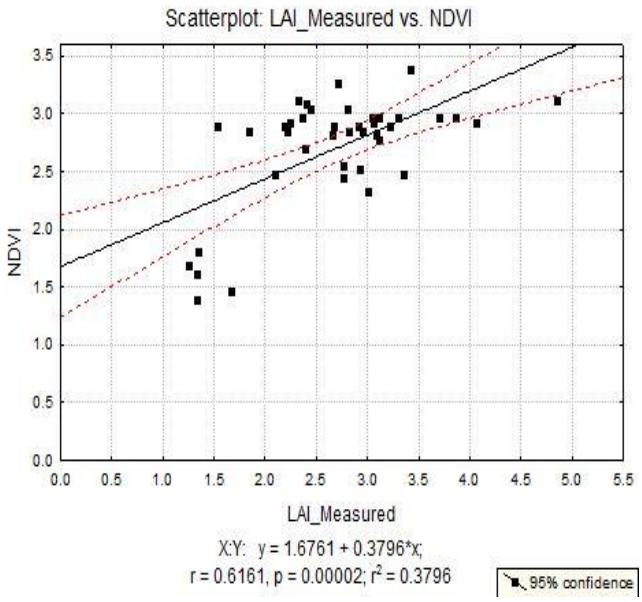

Figure 5.4. Relationships between the best fit vegetation indices (a) GIPVI-LAI, (b) GI-LAI and (c) NDVI-LAI and field measured LAI (m^2m^{-2}) for grass during peak production season of 2014. Black lines represent the best fit functions. *y*=LAI to be estimated, *x*=vegetation index, r = correlation and R^2 =coefficient of determination.

5.3 Performance of RTMs as compared to empirical modelling for estimation of LAI.

In comparison, the inversion of PROSAIL RTM using both ANN and LUT showed to be more accurate than empirical approach (Table 5.5). From Table 5.5, RMSE of 0.138 and intermediate RMSE of 0.265 for LUT confirmed the outperformance of PROSAILH RTM over empirical approach (RMSE of 0.287 was observed from the best fit vegetation index amongst the others). However based on accuracy, LUT-LAI and GIPVI are comparable (LUT-RMSE=0.265 and GIPVI-RMSE=0.287). Generally, inversion of PROSAILH RTM on Landsat 8 could predict grass LAI with high accuracy as compared to empirical modelling.

Table 5.5. Performance comparison between inversion of PROSAILH RTM and empirical approach in estimating LAI using Landsat 8 remote sensing data. [a] R^2 and RMSE of PROSAILH RTM based on LUT inversion approach, [b] R^2 and RMSE of PROSAILH RTM based on ANN inversion approach and [c] R2 aand RMSE of empirical approach of the best fitted vegetation index(GIPVI).

Model	**R^2**	**RMSE**
LUT based inverted PROSAILH RTM[a]	0.5016	0.265
ANN based inverted PROSAILH RTM[b]	0.873	0.138
Empirical approach (GIPVI) [c]	0.465	0.308

Chapter 6: Discussions and conclusion.

6.1 Discussion.

This study was aimed at accuracy assessment of LAI retrieved by the inversion of PROSAILH RTM on Landsat 8 imagery, moreover, to assess the accuracy of PROSAILH RTM when compared to the empirical modelling. For the estimation of LAI using RTMs, LUT and ANN were used to invert the models. While empirical modelling was performed by evaluating Landsat 8 derived vegetation indices using linear regression and bootstrapping. These techniques were compared based on their retrieval accuracies (R^2 and RMSE). The results showed a high LAI retrieval accuracy of the PROSAILH RTM inverted LAI. The retrieval of grass LAI by ANN yielded low RMSE (0.138), while LUT retrieval yielded RMSE of 0.265. For empirical methods RMSE values ranging from 0.289 to 1.4 were observed amongst all indices used. Thus, comparison between two models shows that LAI retrieval through inversion of PROSAIL RTM outperformed empirical methods.

In comparison to results reported in other studies done at similar vegetation type, such as, Si et al. (2012) (R^2=0.70, RMSE=1.02), Darvishzadeh et al. 2008 (R^2= 0.81 and RMSE= 0.76), Vohland and Jarmer, 2008 (R^2 =0.778 and RMSE=0.857), this study observed high accuracy (RMSE=0.265). However LAI variation was slightly low (50%) compared to 81%, 70% and 77% observed from Si et al. (2012), Darvishzadeh et al. (2008) and Vohland and Jarmer (2008), respectively. However, the current results are comparable to the study done at the South African grass by Cho et al. (2014) with reported LAI variation of 49% (R^2 = 0.49). Generally, this study found that inversion of PROSAILH RTM on Landsat 8 imagery is a better estimator of grass LAI in the savannah landscape compared to empirical approach.

This is in agreement with the study done by Vuolo et al. (2010) which was done on crops using RapidEye data. Vuolo et al. 2010 reported a higher prediction accuracy of the LUT (RMSE=0.64) and ANN (RMSE=0.72) when compared to LAI-WDVI (RMSE=1.14). However, Darvishzadeh et al. (2011) reported comparable predictive power between LUT-LAI and VI-LAI. The uncertainties associated with

LUT inversion could have contributed to the poor performance of the LUT approach when compared to ANN. This includes the following:

(1) Because the accuracy of LUT depends on the a-priori information for parameterization of the model, any uncertainty or error on the parameter values could have a major effect on the model. In this study the parameters used to constrain the models could have also contributed as they were retrieved from studies done on geographic site other than South African savannahs. Therefore, it is crucial to validate this model with accurately estimated parameter of South African savannah grasslands.

(2) The mismatch of the Landsat 8 capturing date with the LAI field measurements could have also contributed to the less accuracy of the LUT inversion. The reflectance used for inversion did not correspond with the LAI field measurements due to the overcast during field work. This might have an effect on the inversion as was also reported in the study done by Si et al. (2012).

In case of the empirical approach, comparison to similar studies shows that the observed correlations in this study are slightly lower. The point raised in this study is that the soil adjusted indices such as such, GOSAVI, OSAVI, GSAVI, and SAVI (Table 5.4) have the least accuracies in comparison to indices classified as ratios based indices NDVI, SR, GIPVI, GI, NG, GRVI, GRARVI, PVI, NR, GDVI, DVI, SIPI and NNIR. Also the results showed that by incorporating green band in the ratio based indices, the accuracy increases as GIPVI, GI, NG, NR and NNIR (Table 5.4) indices have the high accuracies. Furthermore, it was shown that GIPVI and GI accuracies surpassed that of the NDVI, which is consistent with the results o by He et al. 2006. Moreover, it was shown that atmospherically resilience indices (GARI) and VARIgreen (not shown in the table) (Table 5.4) yielded worst correlation amongst other groups of indices used in the study. Although there is some reasonable correlation between most VI used and LAI, this study showed opposite results when compared to other studies done on the similar vegetation type. For instance, Darvishzadeh et al. (2008) observed a linear relationship with R^2 of 0.74 with NDVI, whereas, Turner et al. (1999) reported moderate to the strong relationship (R^2= 0.74) between

of NDVI and grass LAI. In both studies NDVI was able to explain 74 % variance of LAI, while in the current study only 38% LAI variance were explained by NDVI. Moreover, the relationship between SAVI2 and LAI was found to be 0.78 by Darvishzadeh et al. (2008), compared to R^2 of 0.34 observed in this study, whereas, in Turner et al. (1999) a moderate to strong relationship (R^2 of 0.54) between SAVI and LAI was reported. Overall, this study showed less accuracy of the relationship between LAI and vegetation indices derived from Landsat 8 imagery.

However, the relatively lower results in the R^2 values were expected as the remote sensing data used for the extraction of VIs did not correspond to the field work, due to overcast on the days of field work. So cloud free images used in this study are two weeks old in which grass was already starting to senescence. The overall study proved that the NIR bands are affected by heterogeneity (leaf dry matter contents and soil background) of the grass as most of the indices that used NIR did not perform well. However, we think that this could be avoided by using satellite data with sufficient spectral bands such as hyperspectral RS data. Moreover the use of multivariable linear regression that incorporates other independent variables (e.g. surface reflectance data, vegetative indices, climate data and categorical data) needs to be tested for the estimation of LAI heterogeneous grass. In addition, the high reflectance of the green bands as reported in He et al. (2006) was proved, because most of the best fit was observed from indices using green bands (Table 5.4). However, since savannahs are characterized by the different vegetation type the model need to be validated to other vegetation type before it could be used to estimate and map LAI at regional scale for the assessment of savannah status.

6.2 Conclusion.

This study aimed at assessing the accuracy of inversion of PROSAIL RTM in retrieving LAI of grassland in South Africa at Landsat 8 level. The model was compared with empirical in order to assess the accuracy of the models. The potential of inversion of PROSAIL RTM as a tool for LAI estimation with higher accuracy than empirical methods has been also confirmed. However, since savannahs are characterized by the different vegetation type more validation and calibration has to be done for inversion of PROSAIL RTM on Landsat 8 imagery. Because the accuracy of LUT depends mostly on a-priori information which currently depends on the data from the literature, we recommend further field work to accurately measure grass parameters to be used as a-priori for the configuration of LUT. This will also help constrain parameter during model inversion. Because vegetation indices are capable of detecting sparsely and dense vegetated areas, bare soil and water bodies they could be used to further constrain LUTs. Therefore we recommend the use of vegetation indices to constrain LUT to be investigated on Landsat 8 data. Since savannahs are heterogeneous, it is problematic when moderate spatial data are used due spectral signal mixing problem, thus we recommend validation of inversion PROSAIL RTM on high spatial resolution for the estimation of LAI on South African savannahs. Overall the results of this study suggest that inversion of 1-dimensional PROSAIL RTM on Landsat-8 imagery could be implemented to estimate and map LAI at regional scale which could aid in rapid assessment of the status of the savannahs.

References

1. Allen, W.A., Gausman, H.W., Richardson, A.J., and Thomas, J.R. (1969). "Interaction of isotropic light with a compact plant leaf," J. Opt. Soc. Amer., vol. 59, pp. 1376–1379.

2. Bacour C., Baret F., Béal D., Weiss M., and K. Pavageau K. (2006). "Neural network estimation of LAI, fAPAR, fCover and LAI Cab, from top of canopy MERIS reflectance data: Principles and validation," *Remote Sens. Environ.*, vol. 105, pp. 313–325.

3. Badhwar, G.D., R.B. MacDonald, N.C. Metha (1986). "Satellite-derived leaf-area-index and vegetation maps as input to global carbon cycle models-a hierachical approach." Int. J. Remote Sensing, 7, pp. 265-281.

4. Bajwa S.G., Gowda P.H., Leh M. (2008). "Comparing Artificial Neural Network with Least Square regression techniques for LAI retrieval from remote sensing data."Pecora 17-The future of Land imaging going operational. Denver, Colorado.

5. Baret F, Guyot G (1991). Potentials and limits of vegetation indices for LAI and APAR assessment. Remote Sensing of Environment 35, pp.161-173.

6. Boegh, E., Soegaard, H., Broge, N., Hasager, C. B., Jensen, N. O., Schelde, K., and Thomsen, A. (2002): Airborne multispectral data for quantifying leaf area index, nitrogen concentration, and photosynthetic efficiency in agriculture, Remote Sens. Environ., 81, pp.179–193.

7. Boken, V.K. and Chandra, S. (2012). Estimating leaf area index for an arid region using spectral data. African Crop Science Journal, Vol. 20, No. 4, pp. 215 – 22.

8. Bonan, G. B. (1993). Importance of leaf area index and forest type when estimating photosynthesis in boreal forests. Remote Sensing of Environment 43, pp.303-314.

9. Bréda NJJ (2003). Ground based measurements of leaf area index: a review of methods, instruments and current controversies. Journal of Experimental Botany 54 (392), pp.2403-2417.

10. Casa, R., Varella, H., Buis, S., Guérif, M., De Solan, B., Baret, F. (2012). Forcing a wheat crop model with LAI data to access agronomic variables: Evaluation of the impact of model and LAI uncertainties and comparison with an empirical approach. Eur. J. Agron. 37, pp.1–10

11. Casanova, D., Epema, G. F., Goudriaan, J. (1998). Monitoring rice reflectance at field level for estimating biomass and LAI. Field Crops Research 55(1-2), pp.83-92

12. Chen, J.M. & Black, T.A. (1992). "Defining leaf area index for non-flat leaves. Plant, Cell and Environment", 15, pp.421–429.

13. Chen, J.M., Cichlar, J. (1995a). "Plant canopy gap size analysis theory for improving optical measurements of leaf area index". Appl. Opt. 34, pp. 6211–6222.

14. Cho, A.M., Skidmore, A., Fabio Corsi, F., van Wieren S.E., Sobhan, I. (2007). Estimation of green grass/herb biomass from airborne hyperspectral imagery using spectral indices and partial least squares regression. International Journal of Applied Earth Observation and Geoinformation 9, pp. 414–424.

15. Clevers, J. G. P. W., and Verhoef, W. (1991). "Modelling and synergetic use of optical and microwave remote sensing". Report 2: LAI estimation from canopy reflectance and WDVI: a sensitivity analysis with the SAIL model, BCRS Report 90-39, 70 pp

16. Combal, B., Baret, F., Weiss, M., Trubuil, A., Macé, D., Pragnère, A et al. (2002). "Retrieval of canopy biophysical variables from bidirectional reflectance using prior information to solve the ill-posed inverse problem". Remote Sensing of Environment, 84 (1), pp.1–15.

17. Combal B, Baret F, Weiss M, Trubuil A, Macé D, Pragnère A, Myneni R, Knyazikhin Y, and Wang L.(2003a). "Retrieval of canopy biophysical variables from bidirectional reflectance using

prior information to solve the ill-posed inverse problem". Remote Sens. Environ., vol. 84, pp. 1–15.

18. Colombo, R., Bellingeri, D., Fasolini, D., and Marino, C.M. (2003). "Retrieval of leaf area index in different vegetation types using high resolution satellite data." Remote Sensing of Environment 86, pp.120-131.

19. Darvishzadeh R, Skidmore A, Schlerf M, and Atzberger C.(2008a) "Inversion of a radiative transfer model for estimating vegetation LAI and chlorophyll in a heterogeneous grassland". Remote Sens. Environ., vol.112, pp. 2592–2604.

20. Darvishzadeh R., Atzberger C., Skidmore A., Schlerf, M. (2011) "Mapping grassland leaf area index with airborne hyperspectral imagery: a comparison study of statistical approaches and inversion of radiative transfer models". ISPRS J. Photogramm. 66(6), pp.894–906.

21. Darvishzadeh, R., Atzberger, C., Skidmore, A.K., Abkar, A.A. (2009). "Leaf Area Index derivation from hyperspectral vegetation indices and there rededge position". Int.J. RemoteSens.30(23), pp.6199–6218.

22. Darvishzadeh R, Ali A. Matkan A.A, and Ahangar A.D. (2012) "Inversion of a Radiative Transfer Model for Estimation of Rice Canopy Chlorophyll Content Using a Lookup-Table Approach". IEEE Journal of selected topics in applied earth observations and remote sensing, vol. 5, no. 4, pp. 1222-1230.

23. Durbha, S.S., King, R.L., N.H. Younan, N.H. (2007). "Support vector machines regression for retrieval of leaf area index from multiangle imaging spectroradiometer." Remote Sensing of Environment, 107, pp. 348–361.

24. D'Urso, G., Menenti, M., and Santini, A. (1999). "Regional application of one-dimensional water flow models for irrigation management." Agricultural Water Management, Elsevier, 40, pp. 291–302.

25. Fang, H., Liang, S., Kuusk, A. (2003). Retrieving leaf area index using a genetic algorithm with a canopy Radiative transfer model. Remote Sensing of Environment, 85 (3), pp. 257–270.

26. Fang H.L. & Liang S.L. (2003).Retrieving Leaf Area Index with a Neural Network Method: Simulation and Validation. IEEE Transactions on Geoscience and Remote Sensing, 41, pp. 2052-2062.

27. Friedl, M.A., Michaelsen, J., Davis, F.W., Walker, H. and Schimel, D.S. (1994). "Estimating grassland biomass and leaf area index using ground and satellite data." Int. J. Remote Sens. 15, pp. 1401-1420.

28. Gascon F., Gastellu-Etchegorry J.P., Leroy M. (2007). "Using multi-directional high-resolution imagery from POLDER sensor to retrieved leaf area index." International Journal of Remote Sensing, vol, 28, 1, pp 167-181.

29. Gao, X., Huete, A., Ni, W., and Miura, T. (2000). "Optical–biophysical relationships of vegetation spectra without background contamination." *Remote Sensing of Environment*, *74*(3), pp. 609-620.

30. Giordano L. (2007). "Mediterranean vegetation monitoring by remotely sensed data: LAI retrieval and vegetation trend analysis within two forested areas in southern Italy." PHD thesis, Retrieved June 11 2013 from *http/ veprints.unica.it/262/1/giordano_ludovica.pdf*.

31. Gobron, N., Pinty, B., and Verstraete, M.M. (1997). "Theoretical limits to the estimation of the leaf area index on the basis of visible and near-infrared remote sensing data." IEEE Transactions on Geoscience and Remote Sensing, Vol. 35, pp. 1438–1445.

32. Goel, N.S., Thompson, R.L. (1984). "Inversion of vegetation canopy reflectance models. IV. Total inversion of the SAIL model." Remote Sensing of Environment, 15, pp. 237-253.

33. Gong, P., Pu R., Biging, G & Larrieu, M. (2003). "Estimation of forest leaf area index using vegetation indices derived from Hyperion hyperspectral data." IEEE Transactions on Geoscience and Remote Sensing, 41, pp. 1355-1362.

34. Gonzalez-Sanpedro, M.C., Toan, T.L., Moreno, J.F., Kergoat, L., Rubio, E. (2008). "Seasonal variations of Leaf Area Index of agricultural fields retrieved from Landsat data." Remote Sensing of Environment, 12, pp.810-824.

35. Haboudane, D., Miller, J. R., Tremblay, N., Pattey, E., Vigneault, P. (2004). "Estimation of leaf area index using ground spectral measurements over agricultural crops: Prediction capability assessment of optical indices." XXth ISPRS Congress:"Geo-Imagery Bridging Continents". Istanbul, Turkey 12-23 July 2004. Commission VII, WG VII/1.

36. Hassan, Q. K., and Bourque, C.P.A. (2010). "Spatial Enhancement of MODIS-based Images of Leaf Area Index." Application to the Boreal Forest Region of Northern Alberta, Canada. Remote Sens. 2, pp. 278-289.

37. He Y, Guo X, and Wilmshurst J, (2006). "Studying mixed grassland ecosystems I: suitable hyperspectral vegetation indices". Can. J. Remote Sensing, Vol. 32, No. 2, pp. 98–107.

38. He Y., Mui, A. (2010). "Scaling up semi-arid grassland biochemical content from the leaf to the canopy level: Challenges and opportunities." Sensors, 10, pp. 11072-11087.

39. Houborg, R. and B. Eva. (2008). "Mapping leaf chlorophyll and leaf area index using inverse and forward canopy reflectance modeling and SPOT reflectance data." Remote Sens. Env.112, pp.186–202.

40. Houborg, R., S. Henrik and B. Eva. (2007). “Combining vegetation index and model inversion methods for the extraction of key vegetation biophysical parameters using Terra and Aqua MODIS reflectance data.” Remote Sens. Env. 106, pp. 39–58.

41. Huete, A. R., Hua, G., Qi, J., Chehbouni, A., & Vanleeuwen, W. J. D. (1992). “Normalization of multidirectional red and NIR reflectances with the SAVI”. Remote Sensing of Environment, 41, pp. 143−154.

42. Huete, A. R., Liu, H. Q., Batchily, K., & Vanleeuwen, W. (1997). “A comparison of vegetation indices global set of TM images for EOS-MODIS”. Remote Sensing of Environment, 59, pp. 440−451.

43. Hui F., Qingjiu T., Zhenyu J. (2003). “Research and quantitative analysis of the correlation between vegetation index and leaf area index”. Remote Sens. Inf. (2), pp. 10-13.

44. Jacquemoud, S., and Baret, F. (1990). “PROSPECT: A model of leaf optical properties spectra”. Remote Sensing of Environment, 34(2), pp. 75-91.

45. Jacquemoud, S. (1993). “Inversion of the PROSPECT + SAIL canopy reflectance model from AVIRIS equivalent spectra: Theoretical study”. Remote Sensing of Environment, 44(2-3), pp. 281-292.

46. Jacquemoud, S., Baret, F., Andrieu, B., Danson, F., Jaggard, K. (1995). “Extraction of vegetation biophysical parameters by inversion of the PROSPECT + SAIL models on sugar beet canopy reflectance data”. Application to TM and AVIRIS sensors, *Remote Sensing of Environment*, *52*(3), pp. 163-172.

47. Jégo, G., Pattey, E., Liu, J. (2012). “Using Leaf Area Index, retrieved from optical imagery, in the STICS crop model for predicting yield and biomass of field crops”. Field Crops Res. 131, pp. 63–74.

48. Jonckheere, I., Fleck, S., Nackaerts, K., Muys, B., Coppin, P., Weiss, M., & Baret, F. (2004): Review of methods for in situ leaf area index determination. Part I. Theories, sensors and hemispherical photography. Agricultural and Forest Meteorology 121 (1-2), 19–35.

49. Kimes, D., Knyazikhin, Y., Privette, J., Abuelgasim, A., & Gao, F. (2000). "Inversion methods for physically-based models". Remote Sensing Reviews, 18(2), pp. 381-439.

50. Kross. A., McNairn H., Lapen D., Sunohara M., Champagne C. (2015). "Assessment of RapidEye vegetation indices for estimation of leaf area index and biomass in corn and soybean crops". International Journal of Applied Earth Observation and Geoinformation 34, pp 235.

51. Kuusk, A. (1985). "The hotspot effect of a uniform vegetative cover". Soviet Journal of Remote Sensing, 3, pp. 645−658.

52. Le Maire G., François C, K. Soudani, Berveiller D, Pontailler J.Y, Bréda N, Genet H, Davi H, and Dufrêne E. (2008) "Calibration and validation of hyperspectral indexes for the estimation of broadleaved forest leaf chlorophyll content, leaf mass per area, leaf area index and leaf canopy biomass". Remote Sens. Environ., vol. 112, pp. 3846–3864.

53. Li, Z., and Guo, X. (2011). "A suitable vegetation index for quantifying temporal variation of leaf area index (LAI) in semiarid mixed grassland". Canadian Journal of Remote Sensing, 36, pp. 709-721.

54. Liu, J., Pattey, E., Jégo, G. (2012). "Assessment of vegetation indices for regional crop green LAI estimation from Landsat images over multiple growing seasons". Remote Sens. Environ. 123, pp. 347–358.

55. Majeke, B., Van Aardt, J.A.N., Cho, M.A. (2008). "Imaging spectroscopy of foliar biochemistry in

Forestry environments". Southern Forests 70(3), pp. 275-285.

56. Marchant R, (2010). “Understanding complexity in savannas: climate, biodiversity and people”. Current Opinion in Environmental Sustainability, 2, pp. 101–108.

57. Mazumdar, 2011 “Multiangular crop differentiation and LAI estimation using PROSAIL model inversion”. Lethbridge University, MSc Thesis, Retrieved May 15 2013, https://www.uleth.ca/dspace/bitstream/.../mazumdar,%20deepaya.

58. Meroni, M., Colombo, R., and Panigada, C. (2004). “Inversion of a radiative transfer model with hyperspectral observations for LAI mapping in poplar plantations”. Remote Sensing of Environment, 92(2), pp. 195-206.

59. Meienberge, G. (2004).”Canopy biophysical parameter retrieval by inversion of the PROSPECT-SAIL RTMs using three different techniques: an iterative minimization algorithm, a LUT approach and a neural network”. Masters. Thesis University of Zürich, Switzerland. Retrieved June 6 2013 from www.geo.uzh.ch/microsite/rsl.../msc...Gil.../2004_Meienberg_Gil.pdf.

60. Mucina, L., Rutherford, M.C. (2006). “The Vegetation of South Africa, Lesotho and Swaziland”. Strelitzia, Cape Town.

61. Myneni, R. B., Nemani R. R. and Running S. W. (1997b). “Estimation of global leaf area and absorbed PAR using radiative transfer models”. IEEE Transaction on Geoscience and Remote Sensing 35: pp. 1380-1393.

62. Nigam, R., Bhattacharya, B.K., Vyas Swapnil., Oza, M.P. (2014). “Retrieval of wheat leaf area index from AWiFS multispectral data using canopy radiative transfer simulation”. International Journal of Applied Earth Observation and Geoinformation. 32, pp. 173-185.

63. Nguy-Robertson, A., Gitelson, A., Peng, Y., Vina, A., Arkebauer, T., Rundquist, D. (2012). “Green leaf area index estimation in maize and soybean: combining vegetation indices to achieve maximal sensitivity”. Agron. J. 104, pp. 1336–1347.

64. Nguyen Thi Thu Ha, Smaling, E.M.A. (Promotor), Verhoef, W. (Promotor) and de Bie, C.A.J.M. (assistant promotor). (2013). "Earth observation for rice crop monitoring and yield estimation: application of satellite data and physically based models to the Mekong Delta". e-book. Enschede, University of Twente Faculty of Geo-Information and Earth Observation (ITC), 2013. ITC Dissertation 222, ISBN: 978-90-6164-348-7.

65. Olson, B. E. (1999). "Impacts of Noxious Weeds on Ecologic and Economic Systems in R". Sheley and J. Petroffs, eds., "Biology and Management of Rangeland Weeds": Corvallis, Oregon, Oregon State University Press, pp. 4-18.

66. Pielke, R., Avissar A.R., Raupach, M, Dolman, A.J., Zeng X. B and Denning A.S. (1998). "Interactions between the atmosphere and terrestrial ecosystems: Influence on weather and climate". Global Change Biology 4, pp. 461-475.

67. Qi, J., Kerr, Y.H., Moran, M., Weltz, S.M., Huete, A.R., Sorooshian, S. and Bryant, R. (2000). "Leaf Area Index Estimates Using Remotely Sensed Data and BRDF Models in a Semiarid Region'. Remote Sens. Environ 73, pp. 1830.

68. Ramoelo A. (2012) "Savanna grass quality: Remote sensing estimation from local to regional scale". Ph.D. Thesis, Wageningen University Retrieved March 5 2013 from www.itc.nl/library/papers_2012/phd/ramoelo.

69. Richter, K., Atzberger, C.,Vuolo, F., Weihs, P., D'Urso, G. (2009). "Experimental assessment on the Sentinel-2 band setting for RTM-based LAI retrieval of sugar beet and maize". Can. J. Remote Sens. 35, pp. 230-247.

70. Running, Steven W, and E Raymond Hunt. (1993). "Generalization of a forest ecosystem process model for other biomes, BIOME-BGC, and an application for global- scale models". Scaling physiological processes: Leaf to globe: pp. 141-58.

71. Sarlikioti, V., Meinen, E., Marcelis, L. F. M. (2011). “Crop Reflectance as a tool for the online monitoring of LAI and PAR interception in two different greenhouse Crops”. Biosystems Engineering 108(2), pp. 114-120.

72. Schlerf, M., and Atzberger, C. (2006). “Inversion of a forest reflectance model to estimate structural canopy variables from hyperspectral remote sensing data”. Remote Sens.Environ. vol.100, pp. 281–294.

73. Scurlock, J. M. O., G. P. Asner, S. T. Gower. (2001). “Worldwide Historical Estimates and Bibliography of Leaf Area Index, 1932-2000.” ORNL Technical Memorandum TM-2001/268, Oak Ridge National Laboratory, Oak Ridge, Tennessee, U.S.A.

74. Shen, L., He, Y., Guo, X. (2013). “Exploration of Loggerhead Shrike Habitats in Grassland National Park of Canada Based on in Situ Measurements and Satellite-Derived Adjusted Transformed Soil-Adjusted Vegetation Index (ATSAVI)”. Remote Sens. 5, pp. 432-453.

75. Si, Y., Schlerf, M., Zurita-Milla, R., Skidmore, A., Wang, T. (2012). “Mapping spatio-temporal variation of grassland quantity and quality using MERIS data and the PROSAIL model”. Remote Sensing of Environment, 121, pp. 415-425.

76. Stroppiana, D., Boschetti, M., Confalonieri, R., Bocchi, S., Brivio, P.A. (2006). “Evaluation of LAI-2000 for leaf area index monitoring in paddy rice”. Field Crops Res. 99, pp. 167–170.

77. Tripathi R., Rabi, N. S., Vinay, K. S., Tomar, R. K., Debashish, C. and S. Nagarajan, S. (2012). “Inversion of PROSAIL model for retrieval of plant biophysical parameters”. J. Indian Soc. Remote Sens. 40(1), pp. 19-28.

78. Turner, D., Cohen, W., Kennedy, R., Fassnacht, K., & Briggs, J. (1999). “Relationships between leaf area index and Landsat TM spectral vegetation indices across three temperate zone sites”. Remote Sensing of Environment, 70, pp. 2–68.

79. Urrutia, J.A.S. (2010) “Validation of the Leaf Area Index product from MODIS-15 for Rice using a Soil-Leaf-Canopy Radiative Transfer Model: A case study of Seville, Spain”. MSc Thesis, Twente University, Netherland. Retrieved May 8 2013 from www.itc.nl/library/papers_2010/msc/gem/urrutia.pdf.

80. Vina, A. (2004). “Remote estimation of leaf area index and biomass in corn and soybean”. Ebraska University, PhD Thesis, Retrieved May 10 from, www. msu. edu/~vina/ Andres_Vina_ Dissertation. pdf.

81. Vohland M & Jarmer T. (2008). “Estimating structural and biochemical parameters for grassland from spectroradiometer data by radiative transfer modelling (PROSPECT +SAIL)”.International Journal of Remote Sensing, 29:1, pp. 191-209.

82. Vuolo, F., Dini, L., D’Urso, G. (2008). “Retrieval of leaf area index from CHRIS/PROBA data: an analysis of the directional and spectral information content”. International Journal of Remote Sensing, 29, pp. 5063–5072.

83. Vuolo, F., Atzberger, C., Richter, K., D’Urso, G., Dash, J. (2010). “Retrieval of biophysical vegetation products from RapidEye imagery”. ISPRS TC VII Symposium – 100 Years ISPRS, vol. 38. ISPRS, Vienna, Austria, pp. 281–286.

84. Walthall, C., Dulaney, W., Anderson, M., Horman, J., Fang, H., Liang, S. (2004). “A comparison of empirical and neural network approaches for estimating corn and soybean leaf area index from Landsat ETM+ imagery”. Remote Sensing of Environment, 92, pp. 465–474.

85. Wang, Y. (2002). “Assessment of the MODIS LAI and FPAR algorithm: Retrieval quality, theoretical basis and validation”. Ph.D., Geography, Boston University, Boston.

86. Weiss, M., Baret, F. (1999). “Evaluation of canopy biophysical variable retrieval performances from the accumulation of large swath satellite data”. Remote sensing of Environment, 70, pp. 293–306.

87. Weiss, M., Baret, F., Myneni, R. B., Pragnere, A., & Knyazikhin, Y. (2000). “Investigation of a model inversion technique to estimate canopy biophysical variables from spectral and directional reflectance data”. Agronomie, 20, pp. 3−22.

88. Weiss, M., Baret, F., Smith, G. J., Jonckheere, I., Coppin, P. (2004). “Review of methods for in situ leaf area index (LAI) determination”. Part II. Estimation of LAI, errors & sampling. Agriculture of forest meteorology. 121, pp. 37- 53.

89. Welles, J.M. (1990). “Some indirect methods of estimating canopy structure”. Remote Sensing of Environment, 5, pp. 31-43.

90. Wiegand, CL., Richardson, A.J., and Kanemasu, E.T. (1979). “Leaf area index estimates for wheat from Landsat and their implications for evapotranspiration and crop modelling”. Agronomy Journal 71 (2), pp. 336-42.

91. Wittamperuma. I, Hafeez. M, Pakparvar. M, Louis, J. (2012). “Remote-sensing-based biophysical models for estimating LAI of irrigated crops in Murry darling basin”. International Archives of the Photogrammetry, Remote Sensing and Spatial Information Sciences, Volume XXXIX-B8, 2012 XXII ISPRS Congress, 25 August – 01 September 2012, Melbourne, Australia.

92. Xavier, A.C, Vettorazzi, C.A. (2004). “Monitoring leaf area index at watershed level through NDVI from LANDSAT-7/ETM+ data”. Sci. Agric. (Piracicaba, Braz.), v.61, n.3, pp. 243-252.

93. Yang F., Sun., Fang H., Yao Z., Zhang J., Zhu Y., Song K., Wang Z., Hu M. (2012). “Comparison of different methods for corn LAI estimation over northeastern China”. International Journal of Applied Earth Observation and Geoinformation, 18, pp. 462–471.

Appendix A

Calibration data for regression of LAI on VI calculated for Landsat 8 bands.

Plots	LAI	NDVI	SR	GI	EVI	GIPVI	GRA	GOSAVI	GRVI	IPVI	NG	NNIR	NR	OSAVI	DVI	SAVI	GSAVI	GARI	SIPI
PL1	2.2	0.54	3.27	2.32	0.391	0.789	0.079	0.423	3.268	0.758	0.616	0.616	0.196	0.407	0.215	0.906	0.911	6.059	1.16
PL2	2.23	0.53	3.27	2.45	0.335	0.771	0.079	0.433	3.411	0.764	0.624	0.624	0.192	0.421	0.29	1.1	0.815	5.531	1.19
PL3	2.67	0.52	3.17	2.34	0.344	0.78	0.084	0.42	3.346	0.76	0.611	0.622	0.193	0.461	0.19	0.826	0.817	5.464	1.16
PL4	2.37	0.56	3.32	2.56	0.302	0.756	0.111	0.477	3.956	0.81	0.672	0.672	0.157	0.495	0.177	0.784	0.876	5.871	1.1
PL5	2.41	0.59	3.81	2.78	0.377	0.793	0.07	0.518	4.492	0.798	0.661	0.661	0.166	0.472	0.205	0.886	0.922	7.455	1.11
PL6	2.34	0.6	3.68	2.83	0.368	0.784	0.077	0.482	3.894	0.783	0.644	0.644	0.178	0.454	0.221	0.923	0.851	0.851	1.14
PL7	3.07	0.55	3.66	3.03	0.309	0.782	0.08	0.474	4.039	0.778	0.665	0.665	0.182	0.45	0.197	0.858	0.889	6.077	1.17
PL8	3.31	0.56	3.4	2.81	0.335	0.797	0.071	0.465	3.917	0.772	0.649	0.649	0.185	0.44	0.191	0.836	0.862	5.975	1.18
PL9	2.94	0.44	3.35	2.78	0.323	0.792	0.071	0.454	3.815	0.774	0.642	0.642	0.188	0.428	0.181	0.807	0.843	5.919	1.19
PL10	1.86	0.53	3.37	2.76	0.311	0.782	0.076	0.439	3.581	0.769	0.645	0.645	0.189	0.442	0.178	0.792	0.832	5.532	1.2
PL11	2.68	0.54	3.3	2.72	0.331	0.791	0.075	0.45	3.77	0.775	0.639	0.639	0.191	0.427	0.185	0.816	0.854	5.679	1.19
PL12	1.55	0.54	3.35	2.76	0.323	0.789	0.073	0.45	3.742	0.771	0.645	0.645	0.187	0.432	0.199	0.864	0.855	6.063	1.19
PL13	4.86	0.6	3.97	3.27	0.405	0.81	0.077	0.511	4.27	0.799	0.643	0.643	0.191	0.43	0.216	0.91	0.985	5.921	1.15
PL14	3.12	0.56	3.76	3.14	0.345	0.797	0.007	0.471	3.947	0.776	0.674	0.674	0.169	0.492	0.232	0.954	0.845	5.803	1.17
PL15	3.87	0.56	3.69	3.08	0.351	0.801	0.073	0.477	4.014	0.795	0.648	0.648	0.186	0.442	0.199	0.859	0.886	5.774	1.16
PL16	2.82	0.58	3.62	2.76	0.394	0.805	0.075	0.477	4.139	0.781	0.666	0.666	0.172	0.483	0.211	0.894	0.923	5.99	1.15
PL17	3.06	0.56	3.57	2.91	0.364	0.796	0.077	0.478	3.919	0.767	0.651	0.651	0.183	0.455	0.22	0.919	0.923	6.038	1.16
PL18	2.83	0.53	3.29	2.73	0.337	0.789	0.078	0.459	3.74	0.78	0.636	0.636	0.192	0.427	0.189	0.826	0.864	5.529	1.18
PL19	3.72	0.56	3.46	2.89	0.366	0.8	0.079	0.481	3.913	0.774	0.652	0.652	0.183	0.46	0.223	0.928	0.934	5.542	1.17
PL20	3.23	0.54	3.27	2.75	0.348	0.791	0.081	0.474	3.844	0.773	0.646	0.646	0.188	0.447	0.211	0.892	0.895	5.213	1.18
PL21	4.08	0.55	3.33	2.79	0.352	0.792	0.08	0.472	3.838	0.883	0.643	0.643	0.188	0.442	0.207	0.88	0.913	0.597	1.15
PL22	3.13	0.51	3.85	2.5	0.344	0.786	0.089	0.467	3.672	0.776	0.787	0.787	0.102	0.618	0.289	1.138	0.925	4.646	1.17
PL23	2.25	0.55	3.31	2.51	0.425	0.802	0.075	0.495	4.068	0.816	0.641	0.641	0.184	0.447	0.22	0.921	0.958	6.777	1.2
PL24	2.46	0.58	3.79	2.73	0.398	0.793	0.077	0.473	3.85	0.737	0.683	0.683	0.154	0.515	0.234	0.962	0.919	6.243	1.14
PL25	2.78	0.45	2.44	2.13	0.236	0.77	0.068	0.396	3.435	0.771	0.611	0.611	0.218	0.351	0.127	0.605	0.68	5.346	1.26

PL26	2.96	0.53	3.17	2.33	0.275	0.769	0.064	0.402	3.394	0.762	0.633	0.633	0.188	0.44	0.15	0.714	0.727	6.895	1.15
PL27	3.1	0.52	2.33	2.27	0.282	0.784	0.064	0.418	3.636	0.763	0.629	0.629	0.196	0.388	0.149	0.708	0.752	6.875	1.18
PL28	3.1	0.56	2.31	2.24	0.258	0.848	0.042	0.399	3.229	0.739	0.637	0.637	0.198	0.411	0.186	0.827	0.855	6.675	1.15
PL29	2.4	0.49	2.66	2.4	0.294	0.779	0.077	0.428	3.594	0.771	0.613	0.613	0.216	0.369	0.161	0.731	0.799	5.628	1.24
PL30	2.93	0.54	2.97	2.59	0.281	0.776	0.079	0.448	3.784	0.681	0.64	0.64	0.189	0.421	0.176	0.792	0.828	6.676	1.16
PL31	2.11	0.43	2.13	1.98	0.155	0.732	0.073	0.379	3.365	0.678	0.554	0.554	0.259	0.257	0.113	0.547	0.669	6.384	1.36
PL32	2.78	0.42	2.45	2.2	0.244	0.789	0.058	0.38	3.527	0.715	0.544	0.544	0.258	0.303	0.094	0.438	0.597	5.129	1.37
PL33	3.37	0.43	2.29	2.14	0.221	0.775	0.062	0.405	3.755	0.824	0.594	0.594	0.236	0.49	0.102	0.505	0.64	6.728	1.3
PL34	2.73	0.64	3.29	2.98	0.366	0.823	0.527	0.489	4.663	0.822	0.7	0.7	0.149	0.489	0.207	0.917	0.994	5.663	1.11
PL35	3.43	0.67	3.57	3.39	0.398	0.859	0.044	0.535	5.734	0.568	0.699	0.699	0.152	0.119	0.207	0.909	0.837	7.343	1.12
PL36	1.34	0.14	1.81	1.29	0.212	0.696	0.143	0.236	1.772	0.614	0.435	0.435	0.33	0.195	0.051	0.285	0.72	1.817	1.49
PL37	1.27	0.22	1.72	1.18	0.149	0.683	0.169	0.309	2.227	0.618	0.482	0.482	0.302	0.208	0.097	0.446	0.643	1.417	1.69
PL38	1.36	0.25	1.41	1.02	0.179	0.716	0.134	0.355	2.52	0.698	0.484	0.484	0.299		0.124	0.57	0.759	1.094	1.58
PL39	3.02	0.39	1.88	1.78	0.248	0.773	0.094	0.303	2.206	0.59	0.58	0.58	0.249	0.344	0.148	0.662	0.815	3.873	1.18
PL40	1.35	0.2	1.45	1.24	0.129	0.69	0.138	0.429	3.414	0.579	0.469	0.469	0.317	0.161	0.084	0.376	0.619	1.155	1.09
PL41	1.68	0.16	1.39	1.27	0.114	0.688	0.167	0.311	2.2	0.579	0.46	0.46	0.333	0.141	0.083	0.426	0.708	0.511	0.92

Appendix B

Results for accuracy assessment between measured and modelled LAI for different LUTs

LUT size	No of solutions	Statistical parameters	RMSE	R^2
5000	1 best case		0.9766	0.101
	best 50	mean	0.8256	0.144
		median	0.8685	0.24
	best 100	mean	0.8594	0.077
		median	0.8594	0.077
10000	1 best case		0.8873	0.054
	best 50	mean	0.79252	0.124
		median	0.81425	0.115
	best 100	mean	0.79795	0.118
		median	0.79795	0.118
15000	1 best case		0.8671	0.18
	best 50	mean	0.7966	0.199
		median	0.8426	0.145
	best 100	mean	0.7991	0.04
		median	0.7991	0.04
20000	1 best case		0.8612	0.139
	best 50	mean	0.761	0.099
		median	0.8212	0.132
	best 100	mean	0.7671	0.097
		median	0.7671	0.097
25000	1 best case		0.8497	0.122
	best 50	mean	0.7499	0.191
		median	0.7952	0.199
	best 100	mean	0.7473	0.165
		median	0.7473	0.165
30000	1 best case		0.8446	0.099
	best 50	mean	0.739	0.194
		median	0.7838	0.283
	best 100	mean	0.7482	0.16
		median	0.7482	0.16
35000	1 best case		0.8396	0.069
	best 50	mean	0.7274	0.237
		median	0.7691	0.205

	best 100	mean	0.7246	0.05
		median	0.7246	0.05
40000	1 best case		0.8197	0.106
	best 50	mean	0.7088	0.265
		median	0.7601	0.107
	best 100	mean	0.7221	0.304
		median	0.7221	0.304
45000	1 best case		0.7501	0.26
	best 50	mean	0.6837	0.324
		median	0.7374	0.256
	best 100	mean	0.7045	0.204
		median	0.7045	0.204
50000	1 best case		0.6462	0.402
	best 50	mean	0.5734	0.407
		median	0.6345	0.394
	best 100	mean	0.6138	0.337
		median	0.6138	0.337
100000	1 best case		0.429	0.3543
	best 50	mean	0.398	0.480
		median	0.363	0.482
	best 100	mean	0.265	0.501
		median	0.265	0.501

Appendix C

The results obtained from optimization of ANN for retrieval of LAI of grass, OutputTF= Transfer function of the output, T_algorithm= Training algorithm, H_layer= number of hidden layers, Lr=learning rate, B_Epoch=Best epoch, Max_Epoch= Maximum epochs obtained, T_pert =Training set error, V_perf= Validation set error, t_perf= testing set error.

T_algorithm	Output TF	Model	H_layers	Lr	B_Epoch	Max_Epoch	T_perf	V_perf	t_perf
Trainrp	Purelin	ANN1	5	0.05	43	63	0.9499	0.0418	0.0867
		ANN2	10	0.05	31	51	0.9205	0.0937	0.1975
		ANN3	15	0.05	72	102	0.0016	0.0018	0.0016
		ANN4	20	0.05	0	20	0.2914	0.2914	8.4136
		ANN5	25	0.05	86	106	0.0015	0.0093	0.0041

		ANN6	30	0.05	90	110	0.0026	0.0048	0.0012
		ANN7	35	0.05	124	144	0.0013	0.6966	0.0034
		ANN8	40	0.05	116	136	0.0016	0.003	0.001
		ANN9	45	0.05	85	105	0.0013	0.0018	0.0036
		ANN10	50	0.05	69	89	0.0055	0.002	0.0037
		ANN11	5	0.5	74	94	0.0029	0.0035	0.0072
		ANN12	10	0.5	59	79	0.009	0.0028	0.002
		ANN13	15	0.5	85	105	0.0014	0.0007	0.0036
		ANN14	**20**	**0.5**	**68**	**78**	**0.0012**	**0.0018**	**0.0014**
		ANN15	**25**	**0.5**	**75**	**95**	**0.0014**	**0.0007**	**0.0016**
		ANN16	**30**	**0.5**	**72**	**92**	**0.0019**	**0.0017**	**0.0038**
		ANN17	35	0.5	92	112	0.0013	0.0021	0.002
		ANN18	40	0.5	90	110	0.0016	0.0031	0.0059
		ANN19	45	0.5	31	71	0.431	0.1684	0.1597
		ANN20	50	0.5	91	111	0.0016	0.0037	0.0008
		ANN21	5	0.01	0	20			
		ANN22	10	0.01	0	20			
		ANN23	15	0.01	81	101	0.0123	0.013	0.0107
		ANN24	20	0.01	87	107	0.011	0.016	0.0037
		ANN25	25	0.01	116	136	0.0011	0.036	0.026
		ANN26	30	0.01	197	217	0.0012	0.005	0.0032
		ANN27	35	0.01	86	96	0.0011	0.036	0.041
		ANN28	40	0.01	232	252	0.0014	0.0011	0.0025
		ANN29	45	0.01	44	64	0.01	0.0031	4.9176
		ANN30	50	0.01	72	92	0.0046	0.0029	0.0022
		ANN31	5	1	20	60	0.0122	0.0086	0.0139
		ANN32	10	1	0	40	NA	NA	NA
		ANN33	15	1	17	47	0.1	0.35	0.0141
		ANN34	20	1	41	81	0.0155	0.0164	0.0173
		ANN35	25	1	37	77	0.0147	0.0136	0.066
		ANN36	30	1	56	96	0.0123	0.0157	0.0135
		ANN37	35	1	147	187	0.3875	0.042	0.0493
		ANN38	40	1	168	208	0.1468	0.088	0.0268
		ANN39	45	1	198	238	0.0164	0.0168	0.0174
		ANN40	50	1	17	47	0.1	0.0135	0.0141
Trainscg	logsig	ANN41	5	0.05	20	60	0.0122	0.0086	0.0139
		ANN42	10	0.05	0	40	NA	NA	NA
		ANN43	15	0.05	17	47	0.1	0.0035	0.0141
		ANN44	20	0.05	41	81	0.0155	0.0164	0.0073

		ANN45	25	0.05	37	77	0.0147	0.0136	0.0066
		ANN46	30	0.05	56	96	0.0123	0.0057	0.0135
		ANN47	35	0.05	147	187	0.3875	0.0042	0.0493
		ANN48	40	0.05	168	208	0.0468	0.0088	0.0168
		ANN49	45	0.05	198	238	0.0094	0.0168	0.0074
		ANN50	50	0.05			NA	NA	NA
		ANN51	5	0.5	57	97	0.009	0.0147	0.0106
		ANN52	10	0.5	125	165	0.0043	0.0033	0.002
		ANN53	15	0.5	222	262	0.0014	0.0048	0.0027
		ANN54	20	0.5	145	185	0.4979	0.01	0.0229
		ANN55	25	0.5	125	145	0.0014	0.0017	0.0034
		ANN56	30	0.5	130	170	0.0138	0.0059	0.0154
		ANN57	35	0.5	86	206	0.0215	0.0072	0.0256
		ANN58	40	0.5	33	73	0.1129	0.0211	0.049
		ANN59	45	0.5	60	100	0.0412	0.0033	0.041
		ANN60	50	0.5	160	200	0.0143	0.0003	0.0047
		ANN61	5	0.01	142	162	0.0123	0.0339	0.6166
		ANN62	10	0.01	15	35	0.4256	0.0199	0.0378
		ANN63	15	0.01	29	49	0.0112	0.0034	0.0047
		ANN64	20	0.01	79	99	0.0098	0.0036	0.0143
		ANN65	25	0.01	50	70	0.0047	0.0019	0.0497
		ANN66	30	0.01	29	49	0.013	0.014	0.0062
		ANN67	35	0.01	75	95	0.0101	0.0151	0.0108
		ANN68	40	0.01	278	298	0.909	0.0939	0.2165
		ANN69	45	0.01	144	241	0.0098	0.0039	0.645
		ANN70	50	0.01	138	144	0.8943	0.1511	0.2197
		ANN71	5	1	72	92	0.0099	0.0063	0.011
		ANN72	10	1	43	63	0.0098	0.0036	0.0144
		ANN73	15	1	95	116	0.9249	0.3088	0.3298
		ANN74	20	1	68	88	0.008	0.0042	0.5629
		ANN75	25	1	44	64	0.0056	0.0054	0.0505
		ANN76	30	1	157	177	0.0125	0.0056	0.0137
		ANN77	35	1	0	21	-	-	-
		ANN78	40	1	44	64	0.0129	0.0065	0.0106
		ANN79	45	1	57	77	0.0128	0.0036	0.0045
		ANN80	50	1					
Trainscg	Purelin	ANN81	5	0.05	56	75	6.0972	0.0379	0.2013
		ANN82	10	0.05	347	387	0.2687	0.1361	0.1551
		ANN83	15	0.05	102	122	0.769	0.1551	0.268
		ANN84	20	0.05	224	244	1.0128	0.3389	0.5653

ANN85	25	0.05	163	183	0.7661	0.118	0.2161
ANN86	30	0.05	293	313	0.0115	0.0057	0.0544
ANN87	35	0.05	452	473	0.3982	0.0938	0.139
ANN88	40	0.05	552	372	0.5227	0.2575	0.1916
ANN89	45	0.05	518	538	0.4026	0.045	0.1049
ANN90	50	0.05					
ANN91	5	0.5	109	189	2.348	2.7376	2.7012
ANN92	10	0.5	33	103	0.564	0.223	0.225
ANN93	15	0.5	22	42	2.0348	1.7376	2.117
ANN94	20	0.5	354	374	0.0564	0.0219	0.0265
ANN95	25	0.5	154	174	0.0287	0.0395	3.9741
ANN96	30	0.5	126	146	1.2293	0.4305	0.3954
ANN97	35	0.5	52	72	1.0684	0.4009	0.4919
ANN98	40	0.5	105	125	1.0599	0.3492	0.3331
ANN99	45	0.5	212	322	1.324	1.2891	1.2069
ANN100	50	0.5	288	308	0.0946	0.0242	0.318
ANN111	5	0.01	57	77	0.0116	0.0049	6.1215
ANN112	10	0.01	289	309	0.9772	0.1894	0.3244
ANN113	15	0.01	56	76	0.9417	0.4758	0.4178
ANN114	20	0.01	185	205	0.0416	0.0088	0.0194
ANN115	25	0.01	21	41	1.5545	4.9389	1.3351
ANN116	30	0.01	257	277	0.03	0.0111	0.0085
ANN117	35	0.01	25	45	2.2348	2.2807	2.4905
ANN118	40	0.01	58	78	1.0173	0.482	0.3161
ANN119	45	0.01	35	55	2.0697	2.1345	1.537
ANN120	50	0.01	79	99	0.1478	0.1616	8.2269